THE N_3H_3 MOLECULAR SYSTEM AND A COUPLED-CLUSTER EFFECTIVE HAMILTONIAN FOR ELECTRONIC SPECTRA

By

DAVID HUEY MAGERS

A DISSERTATION PRESENTED TO THE GRADUATE SCHOOL
OF THE UNIVERSITY OF FLORIDA IN PARTIAL FULFILLMENT
OF THE REQUIREMENTS FOR THE DEGREE OF
DOCTOR OF PHILOSOPHY

UNIVERSITY OF FLORIDA

1988

U OF F LIBRARIES

To the memory of my father Hughey Mulden Magers

To Tina, Brandon, Mom, and Sylvia

ACKNOWLEDGMENTS

Many people deserve my sincere thanks and appreciation for all the help and encouragement they have given me during my years in graduate school. First and foremost, I wish to thank my family and friends for their love, companionship, and support. Too often, I allowed my work and school-related problems to monopolize my time, but they stood by me and patiently reminded me of what is truly important in life. In particular, I thank my wife Tina for her constant love and for always believing in me, my son Brandon for bringing new joy to my life, my parents Mr. and Mrs. H.M. Magers for their prayers and support and for always being proud of me, and my sister Sylvia for being there when I needed her and for understanding me. Also, I thank my in-laws Mr. and Mrs. Ray Godwin for their love and encouragement; I thank Alan Salter for his friendship through all of the ups and downs of graduate school; and I thank Greg Tacket, Jim Lee, and Kimbrough Simmons for listening to me when I called.

For guiding my research, for sharing his knowledge of many-body theory with me, and for supporting me for five years with a research fellowship, I thank my research advisor Prof. Rodney J. Bartlett. I am also grateful to all the professors of the Quantum Theory Project as well as certain other professors in the Chemistry and Mathematics departments for taking time to share their knowledge with me. In particular, I wish to thank Prof. Michael C. Zerner, whose knowledge

and enthusiasm first led me to consider studying theory, and Prof. James E. Keesling for introducing me to other interesting fields of study.

The present work owes much to many people. I thank Dr. Carl Salter and Dr. Alan Salter for first introducing me to the N_3H_3 project, for helping with initial calculations, and for many useful discussions throughout the course of the study; and I thank Prof. Willis B. Person for many helpful discussions on infrared spectra. With regards to the coupled-cluster effective Hamiltonian and excitation energies, I especially thank Dr. Magnus Rittby for programming the effective Hamiltonian equations.

Other projects which are not contained in this dissertation were, nevertheless, a large part of my graduate research. I was aided by Dr. Robert Harrison on a study of isomers and spectra of C_4, and I assisted David Bernholdt on a follow-up study. I also worked with Dr. James Franz and Dr. Kim Ferris on a theoretical examination of hypervalent sulfur compounds. I thank them all. More recently I have collaborated with John Stanton on a number of projects: the determination of infrared intensities at different levels of theory, a new way to compute quadratic electric dipole moment functions, and studies of the O_3 potential surface. The collaboration continues, and I thank him.

TABLE OF CONTENTS

		Page
ACKNOWLEDGMENTS		iii
ABSTRACT		vi
CHAPTERS		
1	INTRODUCTION	1
	Purpose	1
	Summary of Quantum Chemistry	2
2	THE COUPLED-CLUSTER FORMALISM	12
3	BACKGROUND ON THE N_3H_3 MOLECULAR SYSTEM	33
4	COMPUTATIONAL METHODS AND PROCEDURES FOR STUDYING N_3H_3	41
5	RESULTS AND DISCUSSION OF THE N_3H_3 MOLECULAR SYSTEM	46
	Triaziridine	46
	Triimide	55
	Triazene	64
	Cis-Triaziridine	68
	Cis-Triimide	72
	Hydrogen, Nitrogen, and Ammonia	73
	Relative Energies and Thermochemical Quantities	76
	Vibrational Spectra	82
6	A COUPLED-CLUSTER EFFECTIVE HAMILTONIAN FOR EXCITATION ENERGIES	100
7	EXCITATION ENERGY RESULTS AND DISCUSSION	127
8	CONCLUSION	133
REFERENCES		135
BIOGRAPHICAL SKETCH		140

Abstract of Dissertation Presented to the Graduate School
of the University of Florida in Partial Fulfillment of the
Requirements for the Degree of Doctor of Philosophy

THE N_3H_3 MOLECULAR SYSTEM AND A COUPLED-CLUSTER EFFECTIVE HAMILTONIAN FOR ELECTRONIC SPECTRA

By

David Huey Magers

December, 1988

Chairman: Rodney J. Bartlett
Major Department: Chemistry

The relatively unknown N_3H_3 molecule is investigated, and a new method for calculating electronic vertical excitation energies is developed using the methods and formalism of many-body theory.

The potential energy surface of the N_3H_3 molecular system is studied using ab initio many-body perturbation theory and coupled-cluster methods. Five stable isomers are identified. In decreasing order of stability, these are triazene, triimide, cis-triimide, triaziridine, and cis-triaziridine. The infrared spectra of the principal isomers are predicted at the MBPT(2) level using newly developed analytical second-derivative techniques and compared to SCF predictions. The thermochemical quantities enthalpy, entropy, Gibbs free energy, and heat capacity at constant volume are also computed. The predicted IR spectra and these thermochemical properties should aid experimental attempts to synthesize and isolate these compounds.

In addition, a method for directly calculating electronic excitation energies using a coupled-cluster effective Hamiltonian in an equation-of-motion framework is derived. Initial implementation of the method is achieved with the choice of an excitation operator that includes all single excitations out of the reference function and contains an approximate inclusion of double excitations. The reliability of the method is demonstrated with the computation of the excitation energies for N_2 and the beryllium atom, and subsequent comparison with experimental results and results from other theoretical methods.

CHAPTER 1
INTRODUCTION

Purpose

The determination of electronic and vibrational spectra for molecular systems is one of the most important and interesting uses of quantum chemisty today. The present work focuses on the computation of both of these types of spectra within the theoretical formalism of many-body methods. Calculations of vibrational spectra are employed in a study of the relatively unknown N_3H_3 molecular system to determine which isomers, if any, are truly minimum energy structures. In addition, relative energies and thermochemical quantities are computed. The determination of electronic spectra in the present study involves the derivation and implementation of a method to calculate vertical excitation energies directly using a coupled-cluster effective Hamiltonian in an equation-of-motion framework. Thus, the purpose of this work is to study an interesting molecular system and to develop a new method for calculating electronic excitation energies using the theory and techniques of many-body methods. In order to provide the necessary background for these studies, a summary of quantum chemistry is first presented.

Summary of Quantum Chemistry

If we assume that nuclei and electrons are point masses and neglect relativistic interactions, then, to a good approximation, the molecular Hamiltonian in atomic units is

$$H = -1/2 \sum_{\alpha} \frac{1}{m_{\alpha}} \nabla_{\alpha}^2 - 1/2 \sum_{i} \nabla_{i}^2 + \sum_{\alpha,\beta>\alpha} \frac{Z_{\alpha} Z_{\beta}}{r_{\alpha\beta}} - \sum_{\alpha,i} Z_{\alpha} r_{\alpha i}^{-1} + \sum_{i>j} r_{ij}^{-1} \tag{1.1}$$

where α and β are indicies over the nuclei and i and j are indicies over electrons. The first term is the kinetic energy operator for the nuclei; the second term is the kinetic energy operator for the electrons. The third term is the nuclear repulsion potential energy operator where $r_{\alpha\beta}$ is the distance between nuclei α and β with atomic numbers Z_{α} and Z_{β}, respectively. The fourth term is the potential energy operator arising from the attraction between the electrons and the nuclei where $r_{\alpha i}$ is the distance between nucleus α and electron i. The last term is the electron repulsion potential energy operator, r_{ij} being the distance between electrons i and j. Additional terms coupling electronic and nuclear motion are not explicitly shown.

The wavefunctions and energies of a molecular system are then determined from the time-independent Schrödinger equation:

$$H\Psi = E\Psi \ .$$

Unfortunately, exact solutions to this Schrödinger equation are impossible for all but the simplest of systems. Fortunately, a

simplifying approximation which is highly accurate in many situations may be used. The fixed-nuclei or Born-Oppenheimer approximation relys on the fact that electrons move much faster than nuclei. Therefore, in the Born-Oppenheimer approximation nuclei are presumed to be motionless. Thus, we may disregard the kinetic energy operator in Equation 1.1 and treat the nuclear repulsion term as a constant. We are then left with the electronic Hamiltonian

$$H_{el} = -1/2 \sum_i \nabla_i^2 - \sum_{\alpha,i} Z_\alpha r_{\alpha i}^{-1} + \sum_{i>j} r_{ij}^{-1}, \qquad (1.2)$$

and the corresponding Schrödinger equation:

$$H_{el}\psi = E_{el}\psi \, . \qquad (1.3)$$

The total energy of the molecular system is then obtained by adding the nuclear repulsion energy to E_{el}.

Most research today in electronic structure theory involves trying to solve Equation 1.3, and different methods for doing so will be discussed. However, first assume that the electronic Schrödinger equation has already been solved. Nuclear motion can now be considered. According to the Born-Oppenheimer approximation, the electrons move much faster than the nuclei; when the nuclei change their configuration slightly, the electrons immediately adjust to the change. Thus, as the nuclei move, the electronic energy varies smoothly as a function of the parameters defining the nuclear conformation. Different conformations of the molecule may be taken, and Equation 1.3 solved for each one. This allows the construction of a potential energy surface which shows the dependence of the total energy of the molecule on its conformation. The equilibrium geometry

of the molecule corresponds to the minimum of the curve of the surface.

Consider a diatomic molecule and let the equilibrium bond distance be denoted by R_e. When the distortion $\zeta = R - R_e$ is small, the potential energy (V) of the molecule can be expressed as the first few terms of a Taylor expansion:

$$V(\zeta) = V(0) + \left(\frac{dV}{d\zeta}\right)_0 \zeta + \frac{1}{2}\left(\frac{d^2V}{d\zeta^2}\right)_0 \zeta^2 + \frac{1}{3!}\left(\frac{d^3V}{d\zeta^3}\right)_0 \zeta^3 + \cdots$$

where the subscript 0 indicates that the derivatives should be evaluated at R_e (ζ=0). V(0) is a constant and may be set to zero, and the first derivative $dV/d\zeta$ is zero at the minimum. The contribution of the third term is proportional to ζ^3 and may be neglected for small ζ as long as $(d^3V/d\zeta^3)$ is not huge. Thus, for small displacements $V(\zeta) = (1/2)k\zeta^2$ where $k = (d^2V/d\zeta^2)_0$. Therefore, vibrational frequencies for a molecule may be calculated by assuming that its potential energy is a harmonic oscillator.

Almost all applications of quantum mechanics to the problem of quantitatively describing molecular electronic structure begin with the choice of a suitable atomic orbital basis set in terms of which the electronic wavefunction is then parameterized. This basis set usually consists of Gaussian-type functions or contracted Gaussian-type functions centered upon the nuclei in the molecular system. After the primitive integrals with respect to this basis set have been calculated, the self-consistent-field (SCF) method is often employed as an procedure for approximately solving the electronic Schrödinger equation. The approximation is the way in which the electron

repulsion (the third term in Equation 1.3) is handled. The SCF procedure determines a set of molecular orbitals, one-electron functions of space and spin, as linear combinations of the atomic orbital basis functions. The SCF ground-state wavefunction represents the n-particle wavefunction of the molecular system as an antisymmetrized product (Slater determinant) of n occupied molecular orbitals (n one-electron functions). The expectation value of the electronic Hamiltonian over this wavefunction defines the SCF energy, which is the lowest energy that can be obtained from any single-determinantal wavefunction for the given atomic orbital basis set.

The SCF method defines molecular orbitals and is thus central to the molecular orbital approximation which is used by chemists everywhere. The molecular orbital approximation is also known as the Hartree-Fock approximation after Hartree, who introduced the SCF procedure in 1928, and Fock, who introduced the necessary antisymmetry to the orbitals in 1930. In fact, an SCF calculation is often referred to as a Hartree-Fock calculation, but a true Hartree-Fock calculation employs a complete basis set. In other words, the self-consistent-field procedure in a true Hartree-Fock calculation is done numerically, and therefore limited to atoms and diatomics. The method for representing molecular orbitals as linear combinations of atomic basis functions was proposed by Roothaan in 1951.[1]

In the SCF model, each electron moves in its own effective potential, which is a combination of the coulombic repulsion from the average motion of the other electrons and the coulombic attraction from the nuclei. "Correlated" methods are types of calculations which attempt to correlate the motion of the electrons with each other by going beyond the single-determinantal description of the electronic

wavefunction and the effective Hamiltonian used in the SCF method. Since the SCF procedure suffers in accuracy for many properties of interest for many molecular systems, such correlated methods are necessary for reliability and predictibility.

The molecular orbitals determined in the SCF procedure are of two types: "occupied" orbitals and "unoccupied" or "virtual" orbitals. The virtual orbitals in conjunction with the SCF ground-state wavefunction are used to define "excited" determinants which can be used in correlated methods to define multi-determinantal wavefunctions. The set of singly excited determinants (or singles) comprises all determinants obtained by replacing one occupied orbital in the SCF ground-state determinant with a virtual orbital. The collection of all determinants obtained by replacing two occupied orbitals with two virtuals in the SCF determinant compose the doubly excited determinants (or doubles). Triple and higher excitations out of the SCF reference determinant are defined analogously.

Of the correlated methods, perhaps the best known is the method of configuration interaction (CI).[2] This method involves the construction and diagonalization of the matrix representation of the electronic Hamiltonian in the space of all excited determinants. Thus, the CI electronic wavefunction is a linear combination of the SCF reference determinant and all the excited determinants, and therefore is the best possible wavefunction in the space of the determinants. The CI wavefunction is said to be fully correlated, and the corresponding electronic energy contains all of the correlation energy for the molecular system with respect to the initial choice of the atomic basis set.

Unfortunately, the "full" CI method just described is not practical for most molecular systems due to the number of excited determinants. This number is approximately n! for n atomic basis functions. Thus, it is impossible to calculate the total correlation energy for most molecular systems, even with relatively small basis sets. Therefore, procedures for determining most of the correlation energy for a given molecular system are employed.

One such method is truncated CI. This procedure is the same as the full CI one except that the basis set of the Hamiltonian in the correlated calculation is truncated to include only certain types of excited determinants. For example, if only doubly excited determinants are included, the model is known as CID; if singles and doubles are included, the model is called CISD. Eigenvalues and corresponding eigenvectors from the truncated CI Hamiltonian matrix are extracted, yielding the energy and the electronic wavefunction that are variationally optimal for each state in the truncated space.

Another method for solving the correlation problem which is similar to truncated CI is that of multi-configurational self-consistent-field (MCSCF) theory.[3,4] As in the CI model, the MCSCF wavefunction is a linear combination of a selected set of determinants whose coefficients are variationally optimal. However, the molecular orbital coefficients for each determinant are not fixed by the SCF procedure as they were in the CI calculation. In the MCSCF method these coefficients are also allowed to vary.

Often, the best procedures for overcoming the deficiencies of the SCF model are the many-body methods of many-body perturbation theory (MBPT)[5-10] and coupled-cluster (CC) theory.[7-19] Although these methods are not variational, they possess another attribute of the

full CI model that truncated CI and MCSCF methods do not. Many-body methods are size-extensive. For a method to be size-extensive, the corresponding energy must scale properly with the size of the molecular system. In a size-extensive model, the energy of a systen composed of n identical non-interacting components would be the same as n times the energy of one of the components.[10] Since chemical systems may be fundamentally viewed as composed largely of independent electron pairs, the errors of any method which is not size-extensive can be large.

The correlation problem has been discussed above as one largely concerned with determining the correlation energy. It should be reemphasized that properties other than the energy are also desired. The correlated methods described above not only define a procedure for calculating the correlation energy, but also provide a way of computing multi-determinantal wavefunctions which may be used to compute other properties. In general, the mathematical formulas of a given method provide a framework for deriving equations and procedures for the determination of many different molecular properties of chemical interest. In particular, optimum geometries, vibrational frequencies, and infrared intensities are all computed in this work for N_3H_3 within the formalism of MBPT and CC theory.

Except for the brief mention of multiple roots being obtained from a CI computation, the above discussion has also been limited to the electronic ground state. However, electronic excited states are just as important, in particular in connection with problems in molecular spectroscopy, in ionization processes, and in the detailed study of photochemical reactions.

The most simplistic view of electronic excited states of closed-shell molecules is that they are formed by the promotion of one electron from an occupied molecular orbital to a virtual molecular orbital, as in the earlier description of excited determinants. Thus, implicit in this view is the assumption that the ground-state wavefunction is an SCF Slater determinant. Also implicit is the use of these same SCF molecular orbitals to describe the excited state; that is, the orbitals are constrained to retain their ground-state form. For this reason, this method is often called the frozen orbital approximation. Since it is hardly likely that the molecular orbitals which are consistent for the excited state are the same as those for the ground state, this approximation is almost always too simplistic to be more than qualitatively interesting and a good, simple conceptual picture. Other methods must be employed to obtain quantitative excitation energies.

Researchers who employ primarily CI or perturbation theory to correlate electron interaction often use different SCF reference functions for each excited state of interest. Then a correlated calculation of each state provides a total electronic energy for each from which an energy difference is easily computed. Unfortunately, such a course is extremely costly and time consuming, especially if the molecular system being studied has several excited states of interest. When information on several excited states is desired, a procedure for determining excitation energies for many states at once is needed.

The simplest method beyond the frozen orbital approximation for calculating multiple excitation energies is the mono-excited CI or Tamm-Dancoff approximation (TDA) in which excited states are described

as linear combinations of singly excited determinants.[20] Such a CI matrix does not correlate the SCF reference function, since singly excited determinants do not mix with the SCF reference function as stated in Brillioun's theorem.[21]

Other than TDA calculations, only propagator methods have received much attention in direct excitation energy computation.[22] Propagator methods are many-body techniques whose formalisms rest primarily on Green's functions solutions to inhomogeneous equations of quantum mechanical systems. Propagators may be viewed as being either time-dependent or energy-dependent; one representation is merely the Fourier transform of the other. In the latter form, such methods are ideally suited for determination of ionization potentials, excitation energies, and related quantities.

The simplest of the propagator formalisms for the determination of excitation energies is the random phase approximation (RPA),[23,24] which is also known as the time-dependent Hartree-Fock approximation.[25,26] In the language of configuration interaction, the excited state in an RPA calculation is described as the linear combination of all singly excited determinants with some indirect inclusion of doubles (doubly excited determinants).[20,27] RPA singlet excitation energies are usually better than those obtained with a TDA calculation, but RPA triplet excitation energies are usually too small and often suffer from an instability due to the SCF wavefunction inadequately describing the true ground state. Several higher-order RPA methods exist in which electron correlation is added to correct this problem,[22,28] but reliable answers for molecules of chemical interest are still few.

Coupled-cluster theory has an exceptional record of success on the computation of excitation energies when a different SCF reference function from that of the electronic ground state is used for the excited state in question.[29,30] In view of these successes, a method for the direct computation of excited state energies in the formalism of coupled-cluster theory is desirable. One goal of the present work is to derive such a method and to test its reliability by implementing it. In order to provide the relevant background and introduce several useful definitions, the coupled-cluster formalism for individual states of molecules is first reviewed.

CHAPTER 2
THE COUPLED-CLUSTER FORMALISM

In correlated methods, we seek the solution to Equation 1.3 in the space of the N-electron determinants formed from a basis of orthonormal one-electron orbitals. The solution is built upon an approximate single-determinant wavefunction called the reference function, denoted by Φ or $|o\rangle$. The SCF ground-state determinant is often chosen as the reference function. Thus, the spin orbitals in the N-electron determinants are the molecular orbitals determined during the SCF computation. The reference energy is defined as the expectation value of the Hamiltonian over the reference function:

$$E_{ref} = \int \Phi^* H \Phi \, d\tau .$$

Using Dirac's bracket notation, this relation may be more conveniently expressed as

$$E_{ref} = \langle O|H|O\rangle .$$

In terms of second-quantized operators the electronic Hamiltonian is expressed

$$H = \sum_{p,q} h_{pq} \, p^+q + \frac{1}{4} \sum_{\substack{p,q,\\ r,s}} \langle pq||rs\rangle \, p^+q^+sr . \qquad (2.1)$$

By convention, the indices i,j,k,l... represent the spin orbitals which are occupied in the reference function $|O\rangle$ and are called "hole"

states. The indices a,b,c,d... correspond to the virtual (or unoccupied) spin orbitals which are called "particle" states. The indices p,q,r,s... are unrestricted.

The symbols h_{pq} and $\langle pq||rs\rangle$ in Equation 2.1 represent integrals wherein the one- and two-electron operators of the Hamiltonian act upon the orbital basis functions:

$$h_{pq} = \int \phi_p^*(1) \left(-\frac{1}{2}\nabla_1^2 - \sum_\alpha Z_\alpha r_{\alpha 1}^{-1} \right) \phi_q(1)\, d\tau_1 d\sigma_1$$

$$\langle pq||rs\rangle = \iint \phi_p^*(1)\, \phi_q^*(2) \left(r_{12}^{-1} (1 - P_{12}) \right) \phi_r(1)\, \phi_s(2)\, d\tau_1 d\sigma_1 d\tau_2 d\sigma_2 \,.$$

The variables σ_1 and τ_1 are the coordinates of spin and space of electron number one, respectively. The operator P_{12} is the permutation operator which insures that the integral $\langle pq||rs\rangle$ is antisymmetric with respect to the exchange of p with q or r with s.

The operators p^+ and q are the second-quantized creation and annihilation operators, respectively. Excited determinants are represented in second-quantization by a string of creation and annihilation operators acting on the reference function, whereby an electron in an occupied orbital is "annihilated" and an electron is subsequently "created" in a virtual orbital:

$\{a^+i\}|0\rangle = |S\rangle$ Singly excited determinant

$\{a^+ib^+j\}|0\rangle = |D\rangle$ Doubly excited determinant

$\{a^+ib^+jc^+k\}|0\rangle = |T\rangle$ Triply excited determinant

....

In the previous equation, the brackets enclosing a string of second-quantized operators {ABCD...} denote the normal product of the operators relative to the reference function or Fermi vacuum. The normal product of a second-quantized operator string relative to the Fermi vacuum is defined as the rearrangement of operators such that all particle creation operators (a^+) and all hole annihilation operators (i) are to the left of all particle annihilation operators (a) and all hole creation operators (i^+). This rearrangement may be accomplished by commuting the operators such that {ABCD...} = -{BACD...}. This particular rearrangement is chosen to exploit two of the defining conditions of creation and annihilation operators: $i^+|0\rangle = a|0\rangle = 0$. In other words, an occupied orbital may not be created and an unoccupied orbital cannot be annihilated. These conditions also lead to the following anticommutation relation:

$$[p,q]_+ = p^+q + qp^+ = \delta_{pq} .$$

A contraction of second-quantized operators is defined as

$$\overset{\sqcap}{pq} = pq - \{pq\}.$$

Because of the above anticommutation relation, the only nonvanishing contractions are

$$\overset{\sqcap\sqcap}{i^+j} = \delta_{ij} \quad \text{and} \quad \overset{\sqcap}{ab^+} = \delta_{ab} .$$

Contractions needed to be defined in order to introduce Wick's Theorem, which aids in the conversion of an ordinary second-quantized quantum-mechanical operator into its normal-ordered form.

Wick's Theorem states that a string of second-quantized operators ABCD... equals the normal product of the string plus all possible one-fold contracted normal products, two-fold contracted normal products,..., up to all fully contracted normal products of the string.

$$\begin{aligned} ABCD\ldots = \{ABCD\ldots\} &+ \{\overbracket{A}BCD\ldots\} + \{\overbracket{AB}CD\ldots\} + \{A\overbracket{BC}D\ldots\} + \{AB\overbracket{CD}\ldots\} \\ &+ \text{all other one-fold contracted products} \\ &+ \{\overbracket{A}\,\overbracket{B}CD\ldots\} + \{\overbracket{A}B\overbracket{CD}\ldots\} + \{\overbracket{AB}\,\overbracket{C}D\ldots\} + \{\overbracket{AB\overbracket{CD}}\ldots\} \\ &+ \text{all other two-fold contracted products} \\ &\vdots \\ &+ \text{all fully contracted products} \end{aligned}$$

Due to $\overbracket{i^+j}$ and $\overbracket{ab^+}$ being the only nonvanishing contractions, the expectation value of a second-quantized operator string over the reference function can be evaluated by considering only the fully contracted products.

$$\langle 0|ABCD\ldots|0\rangle = \text{(all fully contracted products)}$$

The expectation value of a normal product or a partially contracted normal product over the Fermi vacuum is zero.

$$\langle 0|\{ABCD\ldots\}|0\rangle = 0$$

$$\langle 0|\{\overbracket{A}BCD\ldots\}|0\rangle = 0$$

The Generalized Wick's Theorem states that a product of operator strings in which some operator strings are already in normal product

form is given as the normal product of the overall string plus the sum of all possible normal products with contractions; however, no contractions between pairs of operators within an original normal product are included. A corollary is that for the expectation value of a product of normal product operators over the reference function, only the fully contracted products survive.

The representation of the Fock operator in the orbital basis is given by the matrix elements

$$f_{pq} = h_{pq} + U_{pq}$$

where U_{pq} is the SCF effective potential.

$$U_{pq} = \sum_{j} \langle pj||qj\rangle$$

Recall the form of the electronic Hamiltonian in second-quantized form given in Equation 2.1. If we add and subtract the SCF effective potential from the right side of that equation we obtain

$$H = \sum_{p,q} h_{pq}\, p^{+}q + \sum_{p,q} U_{pq}\, p^{+}q +$$

$$1/4 \sum_{\substack{p,q,\\ r,s}} \langle pq||rs\rangle\, p^{+}q^{+}sr - \sum_{p,q} U_{pq}\, p^{+}q$$

$$= \sum_{p,q} f_{pq}\, p^{+}q + 1/4 \sum_{\substack{p,q,\\ r,s}} \langle pq||rs\rangle\, p^{+}q^{+}sr -$$

$$\sum_{p,q} U_{pq}\, p^{+}q \,.$$

Now assign the following definitions:

$$f = \sum_{p,q} f_{pq}\, p^{+}q \quad ,$$

$$U = \sum_{p,q} U_{pq}\, p^{+}q \quad , \text{ and}$$

$$W = 1/4 \langle pq||rs\rangle\, p^{+}q^{+}sr \quad .$$

Thus $H = f + W - U$.

The normal product form of one-electron operators such as f and U is equal to the ordinary form of the operator minus its expectation value over the reference function. This relation is due to the only nonvanishing contraction being the fully contracted term with the added condition that p=q=i (some hole state). The same type of relation is not true in general for two-electron operators and, in particular, is not true for W. However, with the use of the above definitions, consider the electronic Hamiltonian:

$$H = H_N + \text{all contracted normal products}$$

$$= f_N + \langle 0|f|0\rangle - U_N - \langle 0|U|0\rangle +$$

$$\frac{1}{4} \sum_{\substack{p,q,\\ r,s}} \langle pq||rs\rangle \Big[\{p^{+}q^{+}sr\} + \{p^{+}\overbracket{q^{+}sr}\} + \{p^{+}\overbracket{q^{+}sr}\} + \{\overbracket{p^{+}q^{+}sr}\} +$$

$$\{\overbracket{p^{+}q^{+}sr}\} + \{\overbracket{p^{+}q^{+}sr}\} + \{\overbracket{p^{+}q^{+}sr}\} \Big]$$

$$= f_N + \langle 0|f|0\rangle - U_N - \langle 0|U|0\rangle + \frac{1}{4} \sum_{\substack{p,q,\\ r,s}} \langle pq||rs\rangle \{p^{+}q^{+}sr\} +$$

$$\sum_{\substack{p,q,\\ j}} \langle pj||qj\rangle \{p^+q\} + \frac{1}{2} \sum_{i,j} \langle ij||ij\rangle$$

$$= f_N + \langle 0|f|0\rangle - U_N - \langle 0|U|0\rangle + W_N + \sum_{\substack{p,q,\\ j}} \langle pj||qj\rangle \{p^+q\} +$$

$$\langle 0|W|0\rangle$$

Note that since $H = f + W - U$ that $\langle 0|H|0\rangle = \langle 0|f|0\rangle + \langle 0|W|0\rangle - \langle 0|U|0\rangle$. Also note that the one-fold contracted product term from W is equal to U_N. Therefore,

$$H - \langle 0|H|0\rangle = f_N + W_N = H_N.$$

Thus the normal-ordered form of the Hamiltonian is simply equal to the ordinary Hamiltonian minus the expectation value of the Hamiltonian over the reference function.

$$H - \langle 0|H|0\rangle = H_N = \sum_{p,q} f_{pq}\{p^+q\} + \frac{1}{4} \sum_{\substack{p,q,\\ r,s}} \langle pq||rs\rangle \{p^+q^+sr\}$$

If we now replace the Hamiltonian in Equation 1.3 with the normal-ordered form of the Hamiltonian, we obtain

$$H_N\psi = (H - \langle 0|H|0\rangle)\psi = (E - E_{REF})\psi = \Delta E\psi \ . \qquad (2.2)$$

If the SCF wavefunction is chosen as the reference function, E_{REF} is the SCF energy, ΔE is the correlation energy, and the normal-ordered Hamiltonian simplifies to

$$H_N = \sum_{i,j} f_{ij}\{i^+j\} + \sum_{a,b} f_{ab}\{a^+b\} + \frac{1}{4} \sum_{\substack{p,q,\\ r,s}} \langle pq||rs\rangle \{p^+q^+sr\},$$

since the matrix elements f_{ai} and f_{ia} are zero for SCF orbitals. For the particular choice of canonical SCF orbitals, we have, by definition, $f_{ij} = \delta_{ij}\varepsilon_i$ and $f_{ab} = \delta_{ab}\varepsilon_a$, where ε_p denotes the molecular orbital eigenvalue of orbital p.

In the present study, the many-body methods of many-body perturbation theory (MBPT) and coupled-cluster (CC) theory are used to approximate the solution to the form of the Schrödinger equation given in Equation 2.2. Both of these methods are size-extensive, which means that the energy scales properly with the size of the system. Although MBPT was developed before CC theory, the two methods are closely related. In fact, CC theory is the infinite-order extension of MBPT with low-order iterations of the CC equations yielding finite-order MBPT solutions.

Coupled-cluster theory is built upon the exponential ansatz; that is, the solution to the Schrödinger equation is

$$\Psi = e^{T}|0\rangle$$

where T is defined by a sum of excitation operators

$$T = T_1 + T_2 + T_3 + \ldots.$$

The excitation operators are given by

$$T_1 = \sum_{i,a} t_i^a \{a^+ i\}$$

$$T_2 = \frac{1}{4} \sum_{\substack{i,j,\\ a,b}} t_{ij}^{ab} \{a^+ i b^+ j\}$$

$$\vdots$$

$$T_n = \frac{1}{(n!)^2} \sum_{\substack{i,j,\ldots \\ a,b,\ldots}} t_{ij\ldots}^{ab\ldots} \{a^+ib^+j\ldots\}$$

$$\vdots \qquad ,$$

where the t-amplitudes are antisymmetrized coefficients to be determined. Substitution into Equation 2.2 yields

$$H_N e^T |0\rangle = \Delta E e^T |0\rangle \ .$$

Multiplying on the left by e^{-T}, the Schrödinger equation becomes

$$e^{-T} H_N e^T |0\rangle = \Delta E |0\rangle \ . \qquad (2.3)$$

This relation can be further simplified by use of the Baker-Campbell-Hausdorff expansion.

Consider two general normal product operators A and B. The Hausdorff expansion of $e^{-A}Be^A$ yields a series of commutators:

$$e^{-A}Be^A = B + [B,A] + 1/2!\ [[B,A],A] + 1/3!\ [[[B,A],A,],A] + \ldots .$$

Since a product of normal product operators can be written as a sum of contracted terms, it follows that a product BA has a "connected" part and a "disconnected" part. In the connected part there is at least one contraction that connects B to A; in the disconnected part there is no such contraction. For a commutator of operators [B,A], the disconnected parts cancel, leaving only the connected parts:

$$[B,A] = BA - AB = (BA)_c - (AB)_c + (BA)_d - (AB)_d = [B,A]_c \ ,$$

where the subscript c denotes connected products and the d subscript indicates disconnected products. Thus the expansion becomes

$$e^{-A}Be^{A} = B + [B,A]_c + 1/2!\ [([B,A]_c),A]_c +$$

$$1/3!\ [([([B,A]_c),A]_c),A]_c + \ldots .$$

Furthermore, if A is an excitation operator, A cannot give rise to a connected contribution when it is to the left of other operators. Consequently, the expansion reduces to the following form:

$$e^{-A}Be^{A} = B + (B,A)_c + 1/2!\ ((B,A)_c,A)_c +$$

$$1/3!\ (((B,A)_c,A)_c,A)_c + \ldots = (Be^{A})_c .$$

Thus Equation 2.3 may be expressed as

$$(H_N e^{T})_c|0\rangle = \Delta E|0\rangle . \qquad (2.4)$$

It is also important to point out that the Hausdorff expansion for $e^{-T}H_N e^{T}$ terminates after the four-fold commutator due to the fact that H_N is at most a two-particle operator.

By projecting Equation 2.4 on the left by $\langle 0|$, we obtain the CC energy expression:

$$\Delta E = \langle 0|(H_N e^{T})_c|0\rangle . \qquad (2.5)$$

The t-amplitudes are determined by solving the set of coupled equations obtained by left projection of the singly, doubly, triply, ... excited determinants (S, D, T, ...):

$$\langle S|(H_N e^{T})_c|0\rangle = 0$$

$$\langle D|(H_N e^{T})_c|0\rangle = 0 \qquad (2.6)$$

$$\langle T|(H_N e^T)_c|0\rangle = 0 \ .$$
$$\vdots$$

In order to evaluate the coupled-cluster energy, the exponential operator is expanded and fully contracted terms are identified. The nonvanishing terms are

$$\Delta E = \langle 0|(H_N(T_1 + T_2 + 1/2\ T_1^2))_c|0\rangle \ . \qquad (2.7)$$

This may be represented algebraically by

$$\Delta E = \sum_{i,a} f_{ia}\ t_i^a + \frac{1}{4} \sum_{\substack{i,j,\\ a,b}} \langle ij||ab\rangle\ (t_{ij}^{ab} + t_i^a\ t_j^b - t_i^b\ t_j^a) \ . \qquad (2.8)$$

Nothing else contributes to the energy. All other clusters may only contribute indirectly by their contribution to t_1 and t_2.

Note that this closed-form solution of the correlation energy represents no new approximation. If all T_n cluster operators are included, the full CI wavefunction and energy are obtained. Hovever, for computational practicality the expansion of T must be truncated. Various coupled-cluster approximations result from different choices of this truncation. If we assume that $T = T_2$, then the coupled-cluster doubles (CCD) model is defined.[12] The CCSD model[15] is specified if we approximate T with $T_1 + T_2$, and the CCSDT model[19] is defined by $T = T_1 + T_2 + T_3$. Various other intermediate, approximate models may be formulated by restricting a particular cluster operator to its linear contributions. For example, the CCSDT-1 model[18] is defined by approximating e^T with $\exp(T_1 + T_2) + T_3$.

Recall that to evaluate integral expressions of normal product operators, only fully contracted normal products involving only

contractions between the normal-ordered components of the operator need to be considered. The identification of all such fully contracted products in the CC amplitude equations and energy expression may be conveniently accomplished with diagrammatic techniques. The resulting diagrams may then be interpreted algebraically using simple rules.[7]

The diagrammatic representation of the operators f_N and W_N which compose H_N are presented in Figure 2.1, and the CC excitation operators T_1, T_2, and T_3 are represented diagrammatically in Figure 2.2. Figure 2.3 presents the diagrams which represent each of the fully contracted products in the CC energy expression, and the diagrammatic equations for the T_1, T_2, and T_3 amplitudes in the CCSDT model are shown in Figures 2.4, 2.5, and 2.6, respectively. The energy and amplitude diagrams are constructed by connecting the operator diagrams from H_N and e^T together to form a given excitation level. Each connection denotes a contraction between the operators. The excitation level of each diagram is specified by the number of pairs of unconnected lines at the top of the diagram. This level matches the excitation of the projected determinant. Thus, all diagrams in the CC energy expression, obtained by left projection of the reference function ($\langle 0|$), have a zero-excitation level. Similarly, the diagrams for the T_1, T_2, and T_3 amplitudes of the CCSDT model have excitation levels of one, two, and three, respectively. The explicit algebraic expressions for the CCSDT model have been presented elsewhere.[18]

The connection between MBPT and CC theory is easier to see if the choice of canonical SCF orbitals as the orbital basis is made. With this choice only the diagonal elements of the terms involving f_N are

nonzero. Therefore, these terms may be taken to the opposite side of the cluster equations, thereby forming equations which may be solved iteratively. In particular, the diagrams 3a and 3b in Figure 2.4 are taken to the other side in the T_1 equation; the diagrams 2a and 2b in Figure 2.5 are moved in the T_2 equation; and in the T_3 equation, diagrams 3a and 3b in Figure 2.6 are taken to the opposite side. Solutions to these equations may be constructed by forming successive iterates of increasing order in the correlation perturbation W_N. Iteration of the cluster equations with subsequent substitution into the energy expression yields the finite-order MBPT energies.

Low-order iterations of the T_2 equations are especially important to the connection of CC theory to MBPT. If all t_2 amplitudes are set to zero in the right side of the T_2 equation, the first iteration of this equation is simply given by diagram 1 in Figure 2.5. The resulting amplitude expression is

$$t_{ij}^{ab}(1) = \langle ab||ij\rangle \; / \; (\varepsilon_i + \varepsilon_j - \varepsilon_a - \varepsilon_b) \; . \qquad (2.9)$$

Inserting this value into the the CC energy expression as given in Equation 2.8 yields the second-order MBPT energy. The SCF energy is complete through first order in W_N; therefore, the MBPT correlation models begin at second order. Notice that the MBPT(2) energy originates from doubly excited determinants only.

The next iteration of the T_2 equation may be carried out by substituting the previously obtained t-amplitudes into the linear terms of the equation. These linear terms are represented by diagrams 2c to 2e of Figure 2.5. This second iteration of the T_2 equation gives rise to the MBPT(3) energy. Once again, only doubly excited determinants are involved; therefore, the CCD model is sufficient to

obtain both the second-order and the third-order MBPT energy. However, the third iteration of the T_2 equation, which gives rise to the fourth order MBPT energy by susequent substitution of the t_2 amplitudes into the CC energy expression, involves more than doubly excited determinants.

The lowest-order iterate of T_1 is obtained by substitution of the first-order iterate of T_2 into diagrams 2b and 2c in Figure 2.4 and subsequently dividing by the orbital eigenvalues derived from diagrams 3a and 3b. Thus, this lowest-order iterate of T_1 is second order in W_N. It then contributes to T_2 by way of diagrams 3a and 3b in Figure 2.5. The second-order iterate of T_2 contributes to the third-order iterate of T_2 through the linear diagrams 2c to 2e of Figure 2.5, and the first-order iterate of T_2 contributes to the third-order iterate by way of the quadratic terms in the T_2 equation which are represented by diagrams 5a to 5d in Figure 2.5. Thus, by allowing only t_1 amplitudes to couple with t_2 amplitudes as in the CCSD model, we obtain the fourth-order MBPT contributions: S(4), D(4), and Q(4). S, D, and Q indicate that the contributions arise from single, double, and quadruple excitations, respectively. The fourth-order MBPT terms included in the CCSD model are, therefore, defined as SDQ-MBPT(4). Note that the quadruples arise from $T^2/2$ in the exponential expansion of T_2; the lowest-order energy contributions from quadruply excited determinants actually arise from the products of doubly excited determinants. True four-body excitations (T_4) occur first in fifth-order MBPT.

Higher iterations of the CCSD equations introduce some effects of triple excitations such as T_2T_1 and $T_1^3/3!$ as well as other contributions to higher orders of MBPT, but the "connected" part of

the triples first appears in fourth order. The lowest-order iterate of T_3 is obtained by substitution of the first-order iterate of T_2 into diagrams 1a and 1b of Figure 2.6 and subsequently dividing by the orbital eigenvalues derived from diagrams 3a and 3b. Thus, this lowest-order iterate of T_3 is second order in V_N just like the lowest-order iterate of T_1. This iterate of T_3 contributes to the third-order iterate of T_2 by way of diagrams 4b and 4c in Figure 2.5. Thus, in the third iteration of the CCSDT equations in which t_3 amplitudes may also couple with t_2 amplitudes, we obtain the complete SDTQ-MBPT(4) approximation.

The coupled-cluster equations have been implemented through CCSDT, but computational limitations often force a restriction to a partial inclusion of T_3 in the CC equations. The asympotic dependence of the CCSD equations scale as N^6 where N is the number of basis functions, but any introduction of triples scales as N^7. The previously mentioned CCSDT-1 model is more specifically defined by truncation of the T_3 cluster equation to diagrams 1a and 1b in Figure 2.6 and by the restriction of T_3 contributions to T_1 and T_2 to the linear terms. That is, T_3 is permitted to contribute to T_1 only through diagram 4 in Figure 2.4 and to T_2 only through diagrams 4a to 4c in Figure 2.5. The lowest-order T_3 approximation is preserved so that the CCSDT-1 model is complete through the fourth-order MBPT energy and the second-order MBPT wavefunction. The CCSD + T(CCSD) model offers another approximation to CCSDT. In this model, converged t_2 amplitudes from the CCSD equations rather than t_2 amplitudes from the first-order iterate of T_2 are used to form the first iterate of T_3 in an attempt to introduce some infinite order character into a T(4) result.

Coupled-cluster theory is usually superior to truncated CI simply due to the higher excitations introduced by the exponential ansatz, but the size-extensive property of MBPT and CC methods may be even more important. This property holds for these methods because the energy expression contains only linked diagrams. Linked diagrams are ones with no closed, disconnected part. Because the equations for the CC amplitudes are connected, the subsequent substitution of the amplitudes into the energy expression always yields closed, connected diagrams.

$f_{pq}\{p^{\dagger}q\} =$

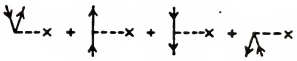

$\langle pq \| rs \rangle \{p^{\dagger}q^{\dagger}sr\} =$

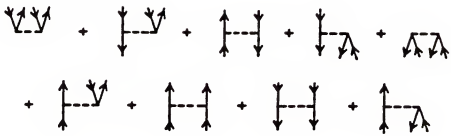

Figure 2.1. The Diagrammatic Representation of H_N.

$t_i^a\{a^{\dagger}i\} =$

$t_{ij}^{ab}\{a^{\dagger}ib^{\dagger}j\} =$

$t_{ijk}^{abc}\{a^{\dagger}ib^{\dagger}jc^{\dagger}k\} =$

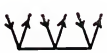

Figure 2.2. The Diagrammatic Representation of Coupled-Cluster Excitation Operators T_1, T_2 and T_3.

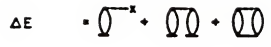

Figure 2.3. The Diagrammatic Representation of the Coupled-Cluster Energy.

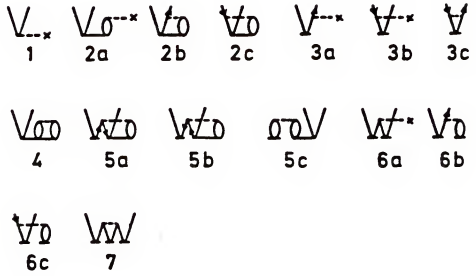

Figure 2.4. The Diagrammatic Representation of the T_1 Amplitude Equation in the CCSDT Model.

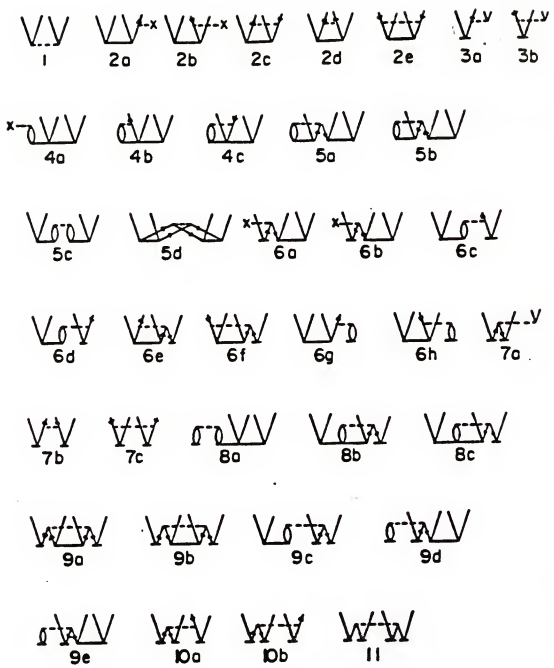

Figure 2.5. The Diagrammatic Representation of the T_2 Amplitude Equation in the CCSDT Model.

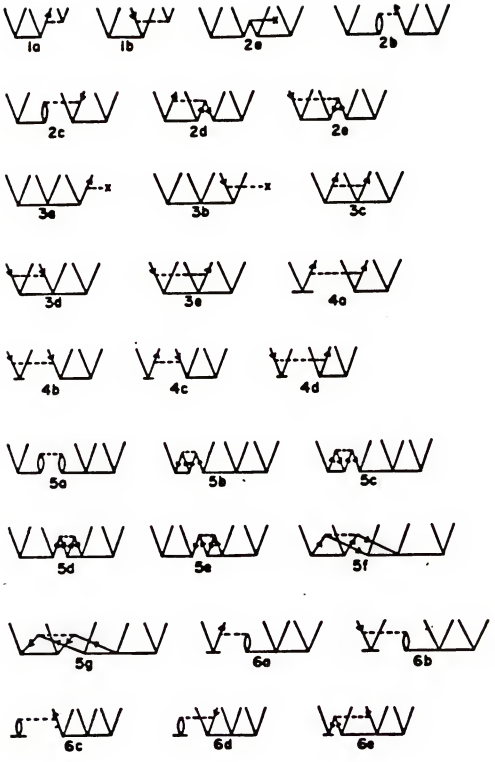

Figure 2.6. The Diagrammatic Representation of the T_3 Amplitude Equation in the CCSDT Model.

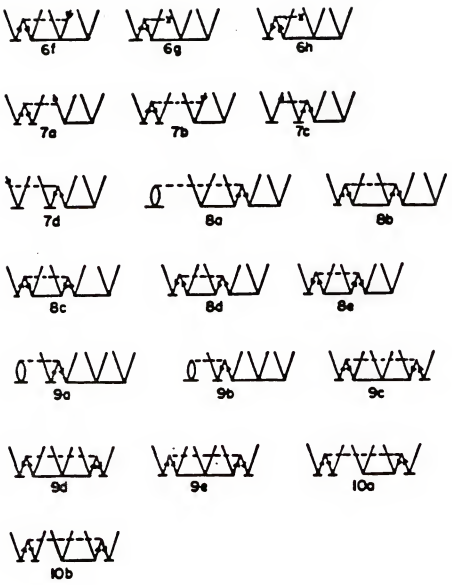

Figure 2.6--continued

CHAPTER 3
BACKGROUND ON THE N_3H_3 MOLECULAR SYSTEM

Chemists have studied small ring compounds such as cyclopropane and cyclobutane for many years. Ring strain makes these systems thermodynamically unstable and kinetically reactive. Thus, their synthesis is particularly challenging. That these compounds also interest kineticists is shown by the fact that the rearrangement of cyclopropane to its open-chain isomer is one of the most-studied unimolecular reactions.[31]

A compound similar to cyclopropane can be imagined, in which the methylene units ($-CH_2-$) are replaced by nitrenes (-NH-). This ring system of nitrogen, which has never been synthesized and isolated, is called triaziridine (1).

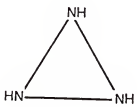

(1)

Triaziridine is a member of a class of inorganic compounds called homocycles, of which the sulfur S_8 is perhaps the best known. Homocycles in general have received little theoretical or experimental

attention; however, triaziridine and its alkyl derivatives have been the subject of some investigations.

In 1977 Kim, Gilje, and Seff[32] reported the serendipitous synthesis of a minute amount of triaziridine on a zeolite crystal in a capillary. They used ammonia in an attempt to reduce the silver ions trapped in a silver-exchanged zeolite, but an X-ray crystal structure of the resulting zeolite indicated the presence of triaziridine facially complexed to the silver ions. The three nitrogen atoms formed an equilateral triangle, but the positions of the three hydrogen atoms could not be determined due to the proximity of the heavy silver atom. The N-N bond length in the ring was 1.49 angstroms, and the length of the Ag-N bond was 2.59 angstroms. Further evidence of the formation of triaziridine came from high resolution mass spectroscopy of the gases exiting the zeolite. Peaks representing both $N_3H_3^+$ and $N_3H_2^+$ were observed while the zeolite was between room temperature and 75° C, suggesting that the N_3H_3 molecule possesses remarkable stability in the gas phase. Despite this observation, neither these investigators nor any other research team has repeated this synthesis of triaziridine.

In spite of this evidence for the formation of triaziridine, there are still many questions about the molecule and its synthesis that remain unanswered. If ammonia is converted to triaziridine, hydrogen gas should be a by-product; but hydrogen was never observed. The silver ions presumably catalyze the conversion, but do they also stabilize the product through complexation? What is the arrangement of the hydrogens in triaziridine? In the zeolite one expects that the hydrogens are located on the side of the ring opposite the silver ion so that charge repulsion is minimized, but this may not be the

structure of the molecule in the gas phase. The mass spectral data suggest that a molecule with empirical formula N_3H_3 is present, but is it triaziridine or one of its isomers?

More recently the synthesis of two alkyl derivatives of triaziridine has been reported by Leuenberger, Hoesch, and Dreiding.[33] They were able to make and isolate 1-(ethoxycarbonyl)-trans-2,3-diisopropyltriaziridine (2) and 2,3-(cis-1,3-cyclopentyl)-1-(methoxycarbonyl)triaziridine (3).

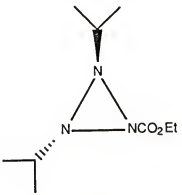

(2)

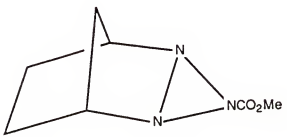

(3)

On standing at room temperature compound 2 thermolyzed to the corresponding azimine (4).

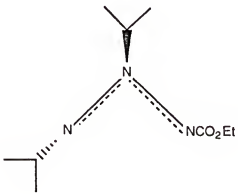

(4)

This reaction proceeded with a half-life of three days. Although one would expect triaziridine itself to be even less stable than an alkyl derivative, this observation is not inconsistent with the stability that Kim et al. observed.

The triaziridine ring structure may not be a minimum on the potential energy surface of N_3H_3. It could, for example, relax directly to triimide (5). This structure is more commonly known as azimine, but I choose to call it triimide to emphasize its similarity to such compounds as diimide and trimethylene.

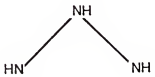

(5)

Another possible structure is triazene (6), which has an N-N double bond.

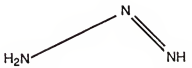

(6)

Triazene has long been thought to be an intermediate in the oxidation of hydrazine.[34] The proposed mechanism includes the formation of hydrazyl radicals (N_2H_3) which combine to form tetrazine (N_4H_6). Triazene and ammonia are then produced from the unimolecular

decomposition of tetrazine. More recent studies by pulse radiolysis have provided further evidence for this mechanism.[35]

Before 1984 only limited investigations of the N_3H_3 surface were reported. In 1973 Lathan et al. reported STO-3G SCF geometries of triaziridine and two of its isomers, cis-triaziridine and triazene.[36] Howell and Kirschenbaum investigated the cis-trans isomerization of triazene about its double bond at the SCF STO-3G level.[37] Hiberty and Leforestier showed that triimide had strong biradical character, in keeping with the expectation that triimide is a 1,3-dipole.[38] Triaziridine was mentioned in a recent paper on inorganic aromaticity by Gimarc and Trinajstić.[39] The arrangement of the six p_z electrons in the π orbitals of the molecule would obey the Huckel 4n+2 rule for aromaticity, and lead to a planar, D_{3h} geometry. However, a simple Huckel calculation or application of Frost's rule revealed that both bonding and antibonding orbitals in the π system are filled, causing the net resonance energy of the π system to be zero. With these qualitative molecular orbital considerations Gimarc and Trinajstić concluded that triaziridine is "not aromatic but saturated" and that the hydrogen atoms will not lie in the plane of the nitrogen ring. This prediction agreed with the structure found earlier by Lathan et al.

Triaziridine is isoelectronic with cyclopropane, which thermally rearranges to propene. This reaction is thought to proceed through an intermediate or transition state known as the trimethylene diradical which is isoelectronic with triimide. The activation enthalpy of this reaction is in the range of 56-65 kcal/mole.[31] The overall enthalpy of reaction to propene is -8 kcal/mole.

Triimide is also isoelectronic with ozone, which has a bent, open structure in its ground state. In the late 1960's and early 1970's theoretical chemists predicted that a cyclic form of ozone would be stable.[40] This conformation of ozone is isoelectronic with triaziridine and cyclopropane. In 1978-79 several good calculations of these two forms of ozone placed the energy difference between them in the range of 20-30 kcal/mole.[41,42] The open form of ozone is more stable due to the contribution of its π system to bonding.

The trimethylene compound of carbon is well-known and cyclic, while the triatomic species of oxygen is well-known and open. However, the trinitrene compound of nitrogen is unknown. Nitrogen lies between carbon and oxygen in the periodic table, so triimide and triaziridine appear to lie in the middle of a trend from cyclic, σ-bonded molecules to open, π-bonded molecules as one moves across the first row from left to right. It is not clear which form of trinitrene is more stable; moreover, the possibility exists that neither form is a local minimum on the N_3H_3 energy surface.

In 1984 Nguyen, Kaneti, Hoesch, and Dreiding addressed these questions.[43] They carried out an SCF investigation of the N_3H_3 surface using two split-valence basis sets, 3-21G and 6-31G. Their geometry optimization of triimide indicated that it is a minimum on the surface, but they did not confirm this by calculating eigenvalues of the force constant matrix. They reported that the energy of triimide is lower than triaziridine's for both basis sets. With the 3-21G basis set, triimide is 10 kcal/mole lower in energy; with the 6-31G basis, this difference increases to 28 kcal/mole.

Nguyen et al. also reported that both triimide and triazene are planar. While this is not surprising for triimide, it is an

interesting result for triazene since it implies that the $-NH_2$ group has flattened to increase the overlap of the unshared pair with the N-N double bond. As Nguyen et al. point out, this result is corroborated by the observation that synthesized derivatives of triazene are planar. Again, however, eigenvalues of the force constant matrix were not computed. They reported triazene to be the most stable isomer. With both basis sets, triazene is 37 kcal/mol lower in energy than triimide.

Further theoretical work on the N_3H_3 system was carried out in 1985 by Carl Salter.[44] His geometry optimizations were also limited to the SCF level of theory, but he used the slightly larger 6-31G* basis set in which polarization functions are added to the nitrogen atoms. Salter also confirmed his geometry minima by computing the eigenvalues of the SCF force constant matrix. The most notable difference in the results of Salter to those of Nguyen et al. is that the optimum structure of triazene is not planar. However, Salter's study of the N_3H_3 molecular system is important because he carried out MBPT(2) single-point calculations of the three isomers at the SCF optimum geometries. His study was the only time electron correlation had been considered. At the MBPT(2) level of theory using the 6-31G* basis set, triazene is 16 kcal/mol lower in energy than triimide, and triimide is more stable than triaziridine by 26 kcal/mol.

The chief goal of these previous theoretical investigations has been to determine the relative electronic energies of the N_3H_3 isomers. Almost all of these studies have been performed at the SCF level only. The one time the effects of electron correlation have been examined was at a low level in single-point calculations. Only

small basis sets have been used in previous investigations, and polarization functions on the hydrogens have never been used during geometry optimizations. Other important aspects of the chemistry of N_3H_3, such as kinetic lability and electronic excitations have not been investigated.

In light of the theoretical and experimental interest in the N_3H_3 system, this system deserves a more extensive theoretical examination. Optimum structures have been found at the correlated level using polarized basis sets. These structures have been characterized by vibrational analysis, which also allows the computation of their infrared spectra. For the most important N_3H_3 isomers, infrared spectra using electron correlation have been determined. The structures and vibrational frequencies of the molecules allow the calculation of their thermochemical properties, including Gibbs free energy. Electronic excitation energies have also been determined for the major isomers. The present goal is to examine aspects of the chemistry of N_3H_3 that current electronic structure theory can address and to do so at a level of ab initio quantum chemistry which allows accurate predictions of the chemical and physical properties of this molecular system.

CHAPTER 4
COMPUTATIONAL METHODS AND PROCEDURES FOR STUDYING N_3H_3

The stability and identification of unknown molecules like N_3H_3 rest upon geometry optimizations that locate minima and transition states and upon accurate predictions of the relative energies of the isomeric forms. Ab initio SCF calculations are frequently helpful in this regard, but predictive accuracy usually demands that electron correlation be included to a high accuracy. Coupled-cluster (CC) theory and its finite-order many-body perturbation theory (MBPT) approximations can often provide this accuracy.

Points of zero force on molecular energy surfaces are located by minimizing first derivatives of the energy with respect to nuclear displacement. These points are subsequently characterized by solving for the eigenvalues of the force constant matrix (the mass-weighted second-derivative matrix). A stable molecular structure is a local minimum on the energy surface; therefore, all the eigenvalues of its force constant matrix will be positive. A transition state is located at a maximum along the reaction path and a minimum for all displacements orthogonal to this path. Thus, one of its eigenvalues will be imaginary. The harmonic vibrational frequencies are related to the eigenvalues of the force constant matrix, and the intensities of the vibrational transitions are related to the derivative of the dipole moment with respect to nuclear displacement. Thus, second derivatives of the energy with respect to nuclear displacement coupled

with first derivatives of the dipole moment give rise to a prediction of the infrared spectrum.

Analytic first and second derivatives of the SCF potential energy surface have been widely available for some time,[45,46] but SCF vibrational frequencies are generally found to be too high compared to experiment by ~10-15%. Analytic first derivatives of the simplest correlated model, MBPT(2), have been available as well,[46] but analytic MBPT(2) second derivatives have become available only recently.[47] Yet, applications of MBPT(2) analytical second derivative methods have already been reported.[29,48] Even though MBPT(2) is the simplest model for the inclusion of electron correlation, it typically accounts for >90% of the basis set correlation energy.[10,49] Consequently, the harmonic frequencies computed at the MBPT(2) level of theory with a reasonable basis set provide a vast improvement over SCF frequencies as they are expected to be within ~5% of experiment.[50]

The three major isomers of N_3H_3, triazene, triaziridine, and triimide, are considered in all of the types of computations performed. Some calculations are also performed on cis-triimide and cis-triaziridine. Each of these cis isomers is less stable than its corresponding trans conformation, so were not considered in the more expensive computations. However, SCF optimum geometries are determined for all five structures using both the DZ and the DZP basis set. The SCF calculations use a single-configuration restricted Hartree-Fock (RHF) wavefunction to represent these closed-shell singlet molecular systems. Two Gaussian-type orbital basis sets are used in all of the calculations: a double-zeta (DZ) basis set and a double-zeta plus polarization (DZP) basis. The DZ basis comprises Dunning's contracted double-zeta bases for hydrogen and nitrogen[51] (a

1.2 scale factor is used in the hydrogen basis); the DZP basis set consists of the DZ basis augmented by the optimum polarization functions (nitrogen d function, exponent =0.902; hydrogen p function, exponent =0.7) of Redmon, Purvis, and Bartlett.[52] This DZP basis set comprises 111 uncontracted basis functions which yield 63 symmetry-adapted basis functions that compose the nitrogen [4s2p1d] and the hydrogen [2s1p] contracted Gaussian set. All calculations on N_3H_3 are performed using the ACES program system.[53]

Single-point correlated calculations are performed on all five isomers using the SCF-DZP optimized geometries at various levels of MBPT and CC theory. No molecular orbitals are frozen in these computations. SCF vibrational frequencies and infrared intensities are also reported for all five isomers at both these geometries and the SCF-DZ optimum geometries. To calculate infrared intensities, the derivative of the dipole with respect to nuclear displacement must be determined. Electric fields for these computations are produced by using point charges.[54]

MBPT(2) optimum geometries and corresponding MBPT(2) vibrational frequencies and infrared intensities for triazene, triimide, and triaziridine are then determined. As with the SCF intensities, the necessary electric fields are produced by point charges. At these correlated optimized geometries, the single-point calculations at various levels of MBPT and CC theory are repeated to yield consistent relative energies. Once again, no molecular orbitals are frozen.

In all of the geometry optimizations of triazene mentioned above, both SCF and MBPT(2), no symmetry constraints are enforced. However, Nguyen et al.[43] reported the optimum geometry of triazene to be planar. Thus, an SCF geometry optimization of triazene is carried out

with ACES using the DZP basis set in which the molecule is constrained to C_s symmetry. The force-constant matrix is calculated and diagonalized to determine if the planar structure is a local minimum on the hypersurface, a transition state, or neither.

Triimide closely resembles the C_{2v} isomer of ozone whose ground state has long been reported to have multireference character.[42,55,56,57] In order to determine if the single-reference description of the ground state of triimide is adequate, generalized valence bond (GVB)[55,58] calculations are performed using ACES. The geometry is optimized at the GVB level of theory, and GVB vibrational frequencies are computed using the DZP basis set. For comparison, single-reference RHF SCF, GVB, and MBPT(2) geometries are also determined for ozone. For these calculations a DZP basis set consisting of Dunning's contracted double-zeta basis for oxygen[51] plus the optimum polarization function of Redmon et al.[52] (oxygen d function, exponent=1.211) is used.

For the purpose of thermochemical comparisons the energies of H_2, N_2, and NH_3 are reported. These molecules are optimized using the DZP basis set at both the SCF and MBPT(2) level of theory. At each set of these DZP optimum geometries, single-point MBPT and CC calculations are performed.

Thermochemical analyses of all N_3H_3 structures are performed using PLOTGIBB.[59] The reference state for N_3H_3 is $\frac{3}{2}(N_2+H_2)$. Thus, to compute heats of formation and free energies, vibrational analyses are carried out on N_2 and H_2. We report thermochemical data at both the SCF level and the MBPT(2) level of theory using the DZP basis set whenever corresponding frequencies are computed. In accordance with the convention that the enthalpies of elements in their standard

states are zero, the enthalpy of nitrogen plus hydrogen is set to zero, and the other enthalpies are shifted accordingly. The temperature-entropy product (TS) is then subtracted from the enthalpies to obtain the free energies.

Finally, vertical excitation energies are determined for the major isomers. With ACES, TDA and RPA excitation energies are computed for triazene, triimide, and triaziridine with the DZ basis set at the SCF-DZ optimum geometries. For comparison, single-point SCF and MBPT(2) calculations of some of the lower triplet states are also performed. Unlike the vibrational spectra, none of these excitation energies can be viewed as quantitative. Often before a molecule enters into a reaction or undergoes a rearrangement, it must first be excited out of its electronic ground state into an excited state. Thus, the goal here is merely to give a qualitative description of the energy range of low-lying electronic excited states for each of the major isomers. In addition, the results from these TDA and RPA calculations are used to discuss some of the advantages and disadvantages of direct excitation energy computations compared to approaches which employ different reference functions.

CHAPTER 5
RESULTS AND DISCUSSION OF THE N_3H_3 MOLECULAR SYSTEM

Triaziridine

Results of the geometry optimizations of triaziridine are given in Table 5.1 along with a figure of the molecule. Triaziridine is found to have a $^1A'$ ground state with C_s symmetry; the SCF electronic configuration is

$$1a'^2 1a''^2 2a'^2 3a'^2 4a'^2 2a''^2 5a'^2 6a'^2 3a''^2 7a'^2 8a'^2 4a''^2.$$

In Table 5.1 the usual shortening of bond lengths with a larger basis set is apparent in the SCF computations, while we observe the usual bond lengthening effect of correlation in the MBPT(2) results. The structure is similar to that reported by Nguyen et al., except that their results have all of the N-N bond lengths equal. In my results the ring is not an equilateral triangle; the N2-N3 bond is slightly longer than the other N-N bonds, even though almost equal at the MBPT(2) level. Even if higher levels of correlation and a better basis set predicted these bond lengths to be equal, the molecule would still have C_s symmetry due to the location of the hydrogens. Nguyen et al. also report that the H5N2N1 angle is equal to the H5N2N3 angle, I find that the H5N2N3 angle is larger. Here, the MBPT(2) geometry gives the largest difference between the angles.

Table 5.1. Optimum Geometries and Electronic Energies of Triaziridine

Bond or Angle	Bond Distances (Å) and Bond Angles in Degrees Basis Set and Level of Theory		
	SCF (DZ)	SCF (DZP)	MBPT(2) (DZP)
N1-N2	1.460	1.414	1.470[a]
N2-N3	1.463	1.418	1.470[a]
H4-N1	1.004	1.004	1.025
H5-N2	1.007	1.006	1.027
Θ(N2N1N3)	60.13	60.19	59.98
Θ(N1N2N3)	59.93	59.91	60.01
Θ(H4N1N2)	108.76	106.23	102.59
Θ(H5N2N1)	108.05	105.78	102.39
Θ(H5N2N3)	112.89	110.10	107.33
Θ(H4N1N2H5)	152.16	155.88	159.58
Θ(N2N3N1H4)	101.34	99.71	97.40
Energy (a.u.)	-164.86620	-164.98666	-165.53732

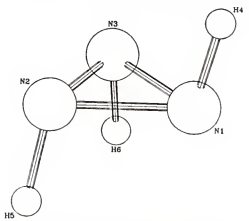

b

a) These two bond lengths differ in the next decimal place.

b) Molecule has C_s symmetry.

The vibrational frequencies and corresponding infrared intensities for triaziridine are reported in Table 5.2. Note that all of the frequencies are real; thus, the structure of triaziridine is a true minimum on the N_3H_3 potential energy hypersurface even at the correlated level. Also, note that a pair of frequencies in the range from 1265 to 1415 wavenumbers are reordered in the change from the smaller to the larger basis set at the SCF level of theory. Both of these vibrational modes have large contributions from the hydrogens bending with respect to the nitrogen ring. It is interesting to note that the 6-31G* results of Salter have the same frequency ordering as the DZ basis results. Neither the DZ basis set nor the 6-31G* basis should be as accurate for frequencies involving such hydrogen motion as the DZP basis because they lack polarization functions on the hydrogens. Studies have shown that SCF frequencies computed with a DZP basis set are usually closer to experimental results than those computed with a either a DZ basis or a 6-31G* basis set for molecules comprising first-row atoms.[50,60]

The SCF intensities for both the DZ and the DZP basis sets are in fair agreement with one exception. The 59.6 km/mol intensity of the 1267 cm^{-1} A′ mode in the DZ results is over one hundred times higher than the SCF-DZP value. Once again this discrepancy is partially due to the lack of hydrogen polarization functions; however, the 6-31G* intensity for this vibrational mode is only 3.52 km/mol. Thus, the lack of nitrogen polarization functions in the DZ basis set is most likely the major cause of this difference. The effect may be indirect, though, arising from the longer bond lengths in the smaller basis set. The longer bond lengths will also affect the values of the

Table 5.2. Vibrational Frequencies and Intensities of Triaziridine

Vibrational Mode	Vibrational Frequencies (cm^{-1}) Basis Set and Level of Theory		
	SCF (DZ)[a]	SCF (DZP)[a]	MBPT(2) (DZP)[a]
A′	3787 (15.9)	3758 (8.85)	3517 (0.943)
A′	3742 (1.94)	3739 (0.710)	3489 (0.758)
A"	3719 (3.59)	3718 (0.205)	3466 (0.326)
A′	1545 (0.382)	1579 (0.233)	1466 (0.142)
A"	1515 (11.6)	1563 (20.3)	1444 (12.1)
A"	1429 (43.9)	1438 (41.3)	1287 (46.3)
A′	1325 (25.0)	1380 (57.8)	1295 (43.9)
A′	1267 (59.6)	1413 (0.318)	1157 (21.2)
A′	1237 (71.4)	1261 (87.0)	1118 (60.2)
A"	1205 (49.3)	1232 (38.8)	1094 (30.6)
A′	854 (32.5)	972 (24.7)	796 (5.18)
A"	847 (33.0)	964 (28.4)	789 (7.62)

[a] Intensities are shown in parentheses in units of km/mole.

vibrational frequencies. Note that all but three of the DZ frequencies are lower than the corresponding DZP values.

SCF theory overestimates the strength of bonding; as a consequence the vibrational frequencies are usually too high. The MBPT(2) model corrects for this shortcoming of SCF theory, lowering the SCF-DZP frequencies by as much as 250 wavenumbers in the N-H stretches of triaziridine. Reordering of frequencies is also common when correlation is included. The same pair of frequencies near 1300 wavenumbers which switched order at the SCF level with the change of basis set, reorder again at the MBPT(2) level of theory. This time a third frequency is also involved in the rearrangement. In general, for molecules of first-row atoms, MBPT(2) frequencies computed with DZP basis sets are usually within 5% of the experimental results (usually within 2% of experimental frequencies computed with harmonic empirical force fields), while frequencies computed at the SCF level using the same DZP basis sets are only within 15%.[50]

Rather than perform the often costly and time-consuming determination of vibrational frequencies at the correlated level, many researchers use a simple scaling factor to lower their SCF frequencies into the experimental range. Obviously, scaling SCF frequencies does not truly correct for correlation effects, because correlation does not affect each frequency by the same amount. Nevertheless, such scaling often yields good agreement with experimental frequencies. On the other hand, computed vibrational intensities cannot be scaled to account accurately for correlation. Note that some of the intensities for triaziridine change only a little with the inclusion of correlation effects while others change dramatically. The relatively strong SCF-DZP intensity of 24.7 km/mol is reduced by a factor of more

than four while the relatively weak SCF-DZP intensity of 0.318 km/mol is increased by a factor of almost 67. Most of the other frequencies differ by less than a factor of two. One study has shown that SCF calculations of infrared intensities using a DZP basis set for molecules comprising first-row atoms yield results which frequently differ from experiment by over 100%. MBPT(2) computations using the same bases yield intensities that are typically within 30% of the experimental values.[50]

Vertical excitation energies for triaziridine are reported in Table 5.3. From these results it is clear that triaziridine has no low-lying electronic excited states. As discussed previously, RPA triplet excitation energies are usually too small, but even the RPA excitation energy for the lowest state, $^3A'$, is over 125 kcal/mol above the ground-state. In the molecular orbital approximation, this $^3A'$ state may be viewed as an excitation of an electron out of one of the doubly occupied asymmetric molecular orbitals into a virtual asymmetric molecular orbital. It is interesting to note that the frozen orbital approximation would not have given a state of this symmetry as the lowest excited state; for even though the highest occupied molecular orbital (HOMO) in the SCF calculation of the ground state singlet is of a" symmetry (i.e., transforms as the a" irreducible representation of the C_s point group), the lowest unoccupied molecular orbital is of a′ symmetry. Therefore, the frozen orbital approximation would predict the lowest electronic excited state to be of A" symmetry.

The TDA and RPA values of Table 5.3 afford us a good example for comparison of the two methods. For all but the highest three triplet states listed, the RPA excitation energy is over 0.4 eV below the

Table 5.3. Vertical Excitation Energies of Triaziridine

Excited State	Vertical Excitation Energies (eV) Level of Theory TDA	RPA	SCF	MBPT(2)
$^3A'$	6.323	5.466	6.156	6.559
$^3A''$	6.836	6.107	6.331	7.246
$^3A'$	7.934	7.505	---	---
$^3A''$	8.069	7.047	---	---
$^1A''$	8.232	8.084	---	---
$^1A'$	8.303	8.164	---	---
$^3A''$	8.844	8.655	8.776	7.745
$^3A''$	9.167	8.951	---	---
$^3A'$	9.234	8.965	8.282	8.174
$^1A'$	9.639	9.552	---	---

Note The calculations for this table were performed with the DZ basis set at the singlet ground state's SCF-DZ optimum geometry.

corresponding TDA value. For the second lowest $^3A''$ state, the discrepancy is over 1.0 eV. However, for all of the singlet excitation energies, the two methods produce results that are within 0.2 eV of each other.

Even though TDA and RPA methods go far beyond the frozen orbital approximation by mixing excited determinants into multi-determinantal wavefunctions to describe the excited states, both methods still use the molecular orbitals from the SCF calculation of the ground state in these determinants. If the exact wavefunction of the excited state is sufficiently different from that of the ground state, the use of these orbitals may be somewhat inadequate. A separate SCF calculation for such an excited state, if possible, allows these orbitals to "relax" in order to provide a better description. Of course, independent MBPT(2) calculations for both the ground state and an excited state should provide an even better energy difference, but when information on many excited states is required, such a course is impractical. From the four triaziridine excited states for which SCF calculations were performed, note that in three out of the four the SCF result lies between the TDA and RPA value. However, for the highest $^3A'$ state reported, the SCF value is almost 0.7 eV below the RPA prediction, and the MBPT(2) result is 0.1 eV below the SCF value. Thus, we may assume that orbital relaxation is especially important for adequately describing this state. The occupation in the SCF reference determinant for this state is equivalent to the excitation of an electron out of a doubly occupied symmetric molecular orbital of the ground state into a symmetric virtual orbital.

The two $^3A''$ excited states for which SCF and MBPT(2) calculations were also performed may too be viewed as simple single electron

excitations out of the ground state. The lowest corresponds to an excitation out of an orbital of a′ symmetry into an orbital of a" symmetry; the other corresponds to the promotion of an electron from an a" symmetry orbital to one of a′ symmetry. Note from the symmetries of the HOMO and LUMO of the SCF ground state calculation that the latter is the triplet state that the frozen orbital approximation would predict to be the lowest in energy. While the MBPT(2) value for this excitation energy is over 0.9 eV below the RPA result and over 1.0 eV below the SCF prediction, the overall ordering of the excited states is unchanged at the MBPT(2) level from the TDA results.

As mentioned above, when information on several excited states is desired, separate SCF and MBPT(2) calculations are impractical. However, keeping the number of separate calculations to a minimum is not the only justification for methods such as TDA and RPA which provide excitation energies for many states at once. In fact, one of the best justifications for such methods is that quite a few of the excited states which may be of interest are almost impossible to study in an independent calculation. For example, consider the second lowest $^3A'$ state in Table 5.3. The largest contribution to its wavefunction is from the determinant formed from an excitation out of the a" HOMO into the lowest virtual orbital of a" symmetry. As has already been pointed out, this determinant is also the major term in the linear expansion of the lowest $^3A'$ state. The difference in the two states arises from the coefficients associated with the other determinants in each expansion. Thus, the convergence of the appropriate SCF calculation to the higher of these two $^3A'$ states

would be quite difficult if not impossible due to the variational collapse of the SCF wavefunction to the state with lower energy.

Triimide

Results of the geometry optimizations of triimide are reported in Table 5.4 along with a figure of the molecule. Triimide has a $^1A_1$ ground state with C_{2v} symmetry, but the assignment of an optimal reference function to describe this ground state is not as clear as with triaziridine. Triimide closely resembles the C_{2v} $^1A_1$ ground state of O_3 whose single-reference RHF SCF electronic configuration is

$$1a_1^2 1b_2^2 2a_1^2 3a_1^2 2b_2^2 4a_1^2 5a_1^2 1b_1^2 3b_2^2 4b_2^2 6a_1^2 1a_2^2,$$

but ozone is not described well by a single reference function. Due to the biradical character of its ground state, O_3 has a second important reference whose configuration is

$$O_3(\text{core})4b_2^2 6a_1^2 2b_1^2.$$

Similarly, the $^1A_1$ ground state of triimide has a single-reference RHF SCF electronic configuration of

$$1a_1^2 1b_2^2 2a_1^2 3a_1^2 2b_2^2 4a_1^2 3b_2^2 5a_1^2 1b_1^2 6a_1^2 4b_2^2 1a_2^2,$$

but the determinant whose configuration is

Table 5.4. Optimum Geometries and Electronic Energies of Triimide

Bond or Angle	Bond Distances (Å) and Bond Angles in Degrees Basis Set and Level of Theory			
	SCF (DZ)	SCF (DZP)	GVB (DZP)	MBPT(2) (DZP)
N1-N2	1.284	1.257	1.278	1.305
H4-N1	1.002	1.009	1.004	1.023
H5-N2	1.013	1.010	1.011	1.033
Θ(N2N1N3)	135.06	135.27	134.11	135.87
Θ(H4N1N2)	112.47	112.37	112.95	112.07
Θ(H5N2N1)	111.14	108.43	108.15	105.35
Energy (a.u.)	-164.90313	-165.00993	-165.05168	-165.58110

a

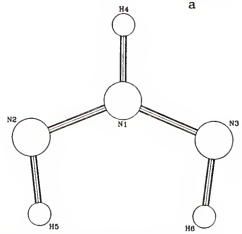

a) Molecule has C_{2v} symmetry.

$$\text{triimide(core)}6a_1^2 4b_2^2 2b_1^2$$

may be too important to limit the description of triimide to single-reference SCF. For convenience, all future references to the above configurations will refer to the primary reference determinant as the a_2 configuration and the secondary reference determinant as the b_1 configuration for both ozone and triimide.

In order to validate the single-reference SCF computations and the MBPT(2) calculations built upon the single-reference SCF function, a generalized valence bond (GVB) geometry optimization of triimide was performed and corresponding GVB vibrational frequencies were computed. Simple GVB calculations such as these are identical to multi-configuration self-consistent-field (MCSCF) calculations limited to two closed-shell configurations. This description is equivalent to an open-shell RHF calculation in which the orbitals are nonorthogonal. The GVB calculation for triimide using the DZP basis set yielded CI-like coefficients of 0.9568 for the a_2 configuration and -0.2906 for the b_1 configuration. By squaring these coefficients and multiplying by two, one may obtain orbital occupancies for the GVB orbitals, which are a measure of the biradical character.[61,57] The orbital occupancy is 1.831 for the a_2 configuration and 0.169 for the b_1 configuration. Thus, in this scheme the RHF single configuration represents 91.5% of the GVB wavefunction which is only somewhat poorer than the 95% for more typical closed-shell ground states. Furthermore, the b_1 configuration is a double excitation out of the a_2 configuration and MBPT(2) correlates the ground state reference with such double excitations. I therefore conclude that the MBPT(2) model is adequate for the geometry, vibrational frequencies, and intensities

of triimide even though the single-reference SCF model may have deficiencies.

In Table 5.4 the similarity of the SCF and GVB values of triimide's internal coordinates is apparent. The fact that the GVB values correspond more closely with the SCF results than with those at MBPT(2) should not be surprising. While it is true that some correlation has been included in the GVB wavefunction, the degree of correlation is much smaller than that obtained at the MBPT(2) level. The additional correlation of the MBPT(2) calculation leads to shorter bond lengths.

The planar structure of triimide allows strong π bonding to take place. The π-structure of triimide is similar to that of the propenyl anion or ozone (see below), with four electrons in the three p orbitals. Salter's 6-31G* Mulliken population analysis of the SCF electronic density shows that the central nitrogen is almost uncharged (-0.06). Nguyen et al. found the central nitrogen had a charge of -0.23 using the same type of SCF population analysis with the 3-21G basis set. The Lowdin population analysis of the SCF-DZP electronic density yields a charge of +0.73 for the central nitrogen atom. All such population analyses are non-physical measurements, yet they provide a means for succinctly summing the physical electronic density into qualitative electronic occupations for each nuclear center. The different types of population analyses rarely differ qualitatively, so we may directly compare them. Thus, we see that the electronic density of the π-system increases on the terminal nitrogens as the basis set is improved.

Another easy way to view the electronic density is to sum the density into bonding regions. Using the SCF bond order scheme of

Natiello et al.,[62] the DZP-SCF N-N bonds for triimide are calculated to have a bond order of 1.74. For triaziridine, the N1-N2 and N1-N3 bonds have a bond order of 1.14, and the bond order of the N2-N3 bond is 1.12. Comparison with the following list of SCF bond orders adds perspective to these N_3H_3 values - ethane: 1.2, benzene: 1.5, and ethene: 2.2.[62] Thus, we see that the N-N bonds in triaziridine are single bonds, and the N-N bonds in triimide are halfway between single and double bonds.

I calculated geometries for O_3 at the single-reference SCF, MBPT(2), and GVB levels so that I could compare the accuracy of each level with known experimental results. The experimental equilibrium bond length r_e is 1.2717 Å and the experimental equilibrium bond angle Θ_e is 116.8°.[63] At the single-reference SCF level, the theoretical value of r_e is 1.1987 Å and the value of Θ_e is 119.2°. The GVB model predicts r_e to be 1.2487 Å and Θ_e to be 115.5°. The coefficients from the GVB calculation were 0.8962 for the a_2 configuration and -0.4437 for the b_1 configuration. These coefficients in turn yield orbital occupancies of 1.606 and 0.394, respectively. We see that ozone exhibits more biradical character than triimide because the single-reference RHF configuration accounts for only 80.3% of the GVB wavefunction. One further indication that an RHF single-reference description of the ground state of triimide is more accurate than an equivalent treatment of the ground state of ozone is that the lowest unoccupied molecular orbital (LUMO) in the single-reference RHF calculation of ozone has negative energy (ε=-0.01023 a.u.), while the energy of the corresponding LUMO for triimide is positive (ε=0.12092 a.u.). Of course, both LUMO's have b_1 symmetry and represent the highest occupied molecular orbitals in the b_1 configurations for each

system. Finally, MBPT(2) computations yield 1.2933 Å as the value for r_e and 116.7° as the value for Θ_e. Thus, we see that good agreement with experiment is obtained at the MBPT(2) level for a system with more biradical nature than triimide.

Vibrational frequencies and intensities for triimide are listed in Table 5.5. In general, the GVB frequencies lie between the SCF and the MBPT(2) values, but three GVB frequencies are actually higher than the corresponding SCF-DZP values. Note that the fifth and sixth vibrational modes reorder from the SCF level when correlation effects are added and that the GVB and MBPT(2) orderings are identical. The largest difference between the SCF and MBPT(2) level is seen in the infrared intensities for the fourth and sixth vibrational modes. These SCF-DZP values are obviously too high; the SCF intensity of 839.3 is over 75 times larger than the corresponding MBPT(2) result. Both values are probably a manifestation of the inadequacy of the single-reference RHF SCF wavefunction. Two of the DZ-SCF intensities are also erroneously large. In this basis these anomalous results correspond to the sixth and seventh vibrational modes. However, note that all of the SCF intensities that are too large are associated with vibrational modes of B_2 symmetry. These B_2 vibrational modes are the asymmetric ones which one would expect to be most affected by the single-reference description of the biradical.

Table 5.6 lists the results of the excitation energy calculations for triimide. Note that the negative triplet excitation energy for the lowest $^3B_2$ state is an example of an RPA triplet instability. Unlike the lowest state for triaziridine, this lowest-lying excited state may be viewed as the promotion of an electron from the HOMO to the LUMO in the frozen orbital approximation. In light of the

Table 5.5. Vibrational Frequencies and Intensities of Triimide

Vibrational Mode	Vibrational Frequencies (cm^{-1}) Basis Set and Level of Theory			
	SCF (DZ)	SCF (DZP)	GVB (DZP)	MBPT(2) (DZP)
A_1	3823 (69.4)	3761 (49.9)	3813	3573 (28.9)
B_2	3672 (30.5)	3701 (19.7)	3686[b]	3435 (11.4)
A_1	3670 (6.59)	3697 (4.67)	3686[b]	3428 (7.10)
B_2	1745 (4.83)	1767 (260.7)	1824	1771 (22.3)
A_1	1644 (16.4)	1673 (7.85)	1644	1517 (16.0)
B_2	1495 (639.6)	1595 (839.3)	1660	1569 (11.1)
B_2	1399 (569.5)	1426 (136.1)	1407	1298 (77.2)
A_1	1292 (27.4)	1389 (24.1)	1338	1163 (11.4)
B_1	1288 (231.0)	1263 (171.9)	1136	1093 (180.2)
B_1	841 (118.3)	896 (88.7)	794	778 (25.7)
A_2[c]	827 (0.00)	823 (0.00)	791	756 (0.00)
A_1	671 (51.7)	706 (47.4)	683	622 (38.0)

a) Intensities are shown in parentheses in units of km/mole.

b) These two calculated frequencies differ in the next decimal place.

c) IR vibrational transition is forbidden by symmetry.

Table 5.6. Vertical Excitation Energies of Triimide

Excited State	Vertical Excitation Energies (eV) Level of Theory TDA	RPA	SCF	MBPT(2)
$^3B_2$	1.267	-3.822	0.453	3.112
$^3A_2$	4.482	4.079	3.640	4.984
$^1A_2$	5.394	5.089	---	---
$^1B_2$	6.250	5.622	---	---
$^3B_1$	6.404	6.191	5.720	6.557
$^1B_1$	7.403	7.292	---	---
$^3A_1$	7.665	6.544	7.470	9.390
$^3A_2$	8.011	7.832	6.839	9.250
$^1A_2$	8.454	8.359	---	---
$^3A_2$	9.034	8.956	---	---

Note The calculations for this table were performed with the DZ basis set at the singlet ground state's SCF-DZ optimum geometry.

importance of the b_1 configuration in which the a_2 HOMO of the SCF ground-state determinant is replaced by the b_1 LUMO, the fact that the $^3B_2$ state coresponding to an excitation out of the HOMO into the LUMO is low in energy is not surprising.

Even though positive, as mentioned before, the energy of the b_1 LUMO of the SCF ground state is small (ε=0.12092). This value is another reason for the small excitation energy to the $^3B_2$ excited state. In fact, the four lowest triplet states for which SCF and MBPT(2) calculations were performed may all be viewed in the molecular orbital approximation as the excitation of an electron into this b_1 symmetry orbital. The lowest $^3A_2$ state corresponds to an excitation out of an orbital of b_2 symmetry, the $^3B_1$ state corresponds to an excitation out of an a_1 symmetry orbital, and the $^3A_1$ excited state corresponds to the promotion of an electron from a b_1 molecular orbital of lower energy than the LUMO.

In Table 5.6, we see that the MBPT(2) excitation energies are higher for all states considered than the results from the other three levels of theory. Once again the biradical nature of the $^1A_1$ ground state is the reason. Because correlation with the b_1 configuration is so important to a proper description of the ground state, the MBPT(2) energy is especially low relative to the SCF energy. Though correlation is also important for the excited states, the effect on the energy is less than for the biradical ground state. The small SCF excitation energy of the $^3B_2$ excited state is also probably due to the inadequacy of the single-determinantal description of the b_1 and a_2 π system. However, if the ground state and the $^3B_2$ excited state are ignored and the lowest $^3A_2$ excited state is used as the reference state, the SCF and MBPT(2) excitation energy values are all within 1.1

eV of each other. Also note, that although differing from the TDA and RPA energy ordering, the SCF and MBPT(2) results predict the same order for the excited states.

Triazene

Table 5.7 contains the optimized internal coordinates for triazene along with a figure of the molecule. The ground state of triazene is ^1A and is well-described by a single-reference closed-shell RHF SCF wavefunction. Using the bond order analysis for triazene, I found the N1-N2 bond to be a double bond (bond order=2.13) and the N2-N3 bond to be a single bond (bond order=1.302), as expected. Both of the DZP optimized geometries, SCF and MBPT(2), are nonplanar, but the SCF-DZ structure essentially does have a plane of symmetry even though it was optimized with no symmetry restraints. Salter reported that the optimum SCF geometries determined with the 6-31G* basis and with the STO-3G basis were nonplanar;[44] the 6-31G and the 3-21G optimized structures of Nguyen et al. were both planar.[43] Salter also reported that the SCF energy difference between the planar conformation and the energetically optimum nonplanar conformation is 2 kcal/mol for the 6-31G* basis set. For the DZP basis set, this difference is 1.3 kcal/mol.

The split-valence basis sets used by Nguyen et al. as well as the DZ basis set that I used favor a planar structure. One would presume this is due to a bias of these basis sets in favor of overlap between the N-N double bond and the unshared pair of electrons on the sp^2 nitrogen atom. Such an overlap would be enhanced by a planar

Table 5.7. Optimum Geometries and Electronic Energies of Triazene

Bond or Angle	Bond Distances (Å) and Bond Angles in Degrees Basis Set and Level of Theory		
	SCF (DZ)	SCF (DZP)	MBPT(2) (DZP)
N1-N2	1.248	1.220	1.274
N2-N3	1.337	1.346	1.365
H4-N1	1.008	1.009	1.029
H5-N3	0.989	0.997	1.012
H6-N3	0.996	1.003	1.021
Θ(N1N2N3)	115.24	113.93	111.59
Θ(H4N1N2)	109.59	106.89	103.82
Θ(H5N3H6)	122.97	115.37	114.81
Θ(H5N3N2)	116.96	111.45	110.52
Θ(H6N3N2)	120.07	114.16	113.57
Θ(H4N1N2N3	180.00	177.25	176.09
Θ(H6N3N2N1)	0.00	20.77	21.21
Energy (a.u.)	-165.96092	-165.05823	-165.60259

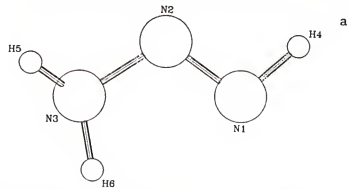

a

a) Molecule has no symmetry in the DZP basis set, but is almost planar in the DZ basis.

structure. However, Nguyen et al. report that the electron pairs in the double bond and on the sp^2 nitrogen are "rather localized." Of course, I observe the same localization in the non-planar DZP structures, but I do not observe as much localization in the planar DZ conformation. Nevertheless, the small overlap that I do observe in the DZP calculations is certainly one of the chief reasons that these optimum structures are as close to planarity as they are.

The vibrational frequencies and intensities of triazene are presented in Table 5.8. Once again we observe a reordering of two of the frequencies, the N1-N2 stretch and the H5-N3-H6 bend, with the inclusion of electron correlation, but for this molecule the SCF-DZP infrared intensities are quite similar to those reported at the MBPT(2) level of theory. Only two differ substantially. However, note how different the SCF-DZ results are from the SCF-DZP values. The agreement between tha two basis sets is especially poor for the intensities corresponding to the vibrational modes representing the out-of-plane deformations of the three hydrogen atoms. The lowest DZ frequency is also of particular interest. Its value is almost 25% below the corresponding SCF-DZP result, and its intensity is much larger than any of the other values, DZ or DZP. This small frequency gives some indication that the energy barrier to an out-of-plane structure is small in the DZ basis set.

I also calculated SCF-DZP frequencies for the planar conformation. I found the planar SCF-DZP conformation to be a transition state; it has a single imaginary frequency of 517i corresponding to the out-of-plane deformation of the hydrogens. Therefore, I expect the harmonic approximation to break down for the lowest frequency mode of vibration

Table 5.8. Vibrational Frequencies and Intensities of Triazene

Vibrational Mode[a]	Vibrational Frequencies (cm^{-1}) Basis Set and Level of Theory		
	SCF (DZ)[b]	SCF (DZP)[b]	MBPT(2) (DZP)[b]
N3-H5 stretch	4037 (79.1)	3914 (38.8)	3731 (34.7)
N3-H6 stretch	3827 (42.9)	3755 (14.7)	3541 (9.35)
N1-H4 stretch	3709 (2.33)	3692 (0.973)	3468 (0.041)
H5-N3-H6 bend	1802 (37.5)	1787 (54.1)	1647 (47.3)
N1-N2 stretch	1744 (197.0)	1873 (103.9)	1540 (46.9)
N2-N1-H4 bend	1596 (8.85)	1615 (6.66)	1476 (6.76)
N2-N3-H5 bend	1335 (71.7)	1389 (48.6)	1262 (44.6)
N2-N3 stretch	1215 (178.9)	1213 (83.4)	1133 (49.4)
H4 out-of-plane deformation	1031 (91.5)	1055 (49.8)	952 (41.6)
H6 out-of-plane deformation	653 (51.3)	717 (353.8)	684 (341.1)
N1-N2-N3 bend	632 (28.1)	679 (5.67)	635 (6.79)
H5 out-of-plane deformation	392 (490.2)	517 (80.8)	501 (83.2)

a) The dominant internal coordinate is used to label each normal mode of vibration.

b) Intensities are shown in parentheses in units of km/mole.

of triazene, due to the presence of a degenerate well separated by a small barrier of 1-2 kcal/mole.

The vertical excitation energies for the lowest-lying electronic excited states for triazene are reported in Table 5.9. Although not as relatively low-lying as the lowest triplet state for triimide, the lowest triplet state for triazene has an SCF excitation energy of less than 58 kcal/mol. Once again, we observe an instability in the RPA calculation of this lowest triplet. Also note the difference in the SCF and MBPT(2) values for the excitation energy of this excited state. Although this difference is not as large as in the triplet excitation energies of triimide, inclusion of electron correlation is obviously important for the ground-state singlet of triazene.

Triazene with its C_1 symmetry offers us a good example of the importance of methods which calculate excitation energies directly. Although the excitation energies of many excited states are easily determined with a TDA or RPA calculation, only the energy of one triplet excited state may readily be calculated in an independent SCF and MBPT(2) computation.

Cis-Triaziridine

Cis-triaziridine, a form of triaziridine with all hydrogens on the same side of the nitrogen ring, was investigated at the SCF level of theory. The predicted geometry and vibrational frequencies and intensities of cis-triaziridine using the DZ and DZP basis sets are shown in Tables 5.10 and 5.11. Cis-triaziridine has C_{3v} symmetry; its ground state configuration is given by:

Table 5.9. Vertical Excitation Energies of Triazene

Excited State	Vertical Excitation Energies (eV) Level of Theory TDA	RPA	SCF	MBPT(2)
^3A	2.927	-2.423	2.513	3.698
^3A	3.368	2.578	---	---
^1A	4.298	4.049	---	---
^1A	7.708	7.295	---	---
^3A	8.279	8.054	---	---

Note The calculations for this table were performed with the $\overline{DZ}$ basis set at the singlet ground state's SCF-DZ optimum geometry.

Table 5.10. Optimum Geometries and Electronic Energies of cis-Triaziridine

Bond or Angle	Bond Distances (Å) and Bond Angles in Degrees SCF Level of Theory Basis Set DZ	DZP
N1-N2	1.467	1.419
H4-N1	1.011	1.007
Θ(N1N2N3)	60.00	60.00
Θ(H4N1N2)	112.39	109.62
Θ(H4N1N2N3)	103.76	101.88
Energy (a.u.)	-164.84116	-164.96860

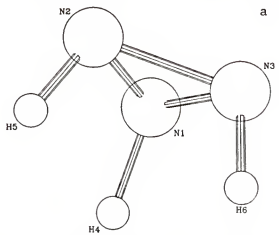

a

a) Molecule has C_{3v} symmetry.

Table 5.11. Vibrational Frequencies and Intensities of cis-Triaziridine

Vibrational Mode	Vibrational Frequencies (cm^{-1}) SCF Level of Theory, Basis Set DZ[a]	Basis Set DZP[a]
A_1	3700 (2.69)	3730 (0.030)
E	3659 (0.213)	3689 (1.38)
	3659 (0.213)	3689 (1.38)
E	1515 (44.0)	1561 (54.8)
	1515 (44.0)	1561 (54.8)
A_1	1368 (0.0012)	1409 (0.449)
A_2[b]	1345 (0.00)	1362 (0.00)
A_1	1252 (0.0407)	1412 (1.47)
E	1186 (2.82)	1206 (4.33)
	1186 (2.82)	1206 (4.33)
E	828 (31.7)	944 (26.3)
	828 (31.7)	944 (26.3)

a) Intensities are shown in parentheses in units of km/mole. Intensities for degenerate vibrational frequencies should be summed to give one value for the mode; for example, the E mode of 3667 wavenumbers in the DZP basis set has an overall calculated intensity of 2.76 km/mole.

b) IR vibrational transition is forbidden by symmetry.

$$1a_1^2 1e^4 2a_1^2 2e^4 3a_1^2 4a_1^2 3e^4 4e^4.$$

The N-N bond lengths in cis-triaziridine are nearly identical to the N_2-N_3 bond length in triaziridine using the same basis sets, while SCF theory predicts that the energy lies 11-16 kcal/mol above triaziridine. Thus, the energy difference is due to the two additional cis hydrogen interactions. Although the cis form of triaziridine is not as stable as the trans form, it is of particular interest since it may more closely resemble the form of triaziridine trapped in the silver-exchanged zeolite by Kim et al.[2]

If the geometry of cis-triaizirdine were optimized at the MBPT(2) level, I would expect the N-N bond distance to be slightly larger than the 1.470 Å bond distance of triaziridine at this level. This bond distance is within 0.02 Å of the experimental N-N bond length that Kim et al. observed. Also, the larger experimental distance could be due to the presence of the silver.

Cis-Triimide

In triimide, the terminal hydrogens lie on the opposite side of the nitrogen ring from the middle hydrogen. Additional conformations of triimide in which one or both terminal hydrogens rotate to the opposite side of the chain are also possible. The cis conformation, where both hydrogens have rotated so that all three hydrogens lie on the same side of the nitrogen chain, was optimized at the SCF level of theory with both the DZ and the DZP basis sets. The predicted geometry and vibrational frequencies and intensities of cis-triimide

are shown in Tables 5.12 and 5.13. Cis-triimide has C_{2v} symmetry; its ground state configuration is

$$1a_1^2 1b_2^2 2a_1^2 3a_1^2 2b_2^2 4a_1^2 5a_1^2 3b_2^2 1b_1^2 4b_2^2 6a_1^2 1a_2^2.$$

As expected the N-N bond distances in cis-triimide are similar to the N-N bond distances in triimide. The energy of the cis confomer is higher due to the increased dipole moment caused by placing the positively-charged hydrogens on one side of the molecule and the negatively-charged nitrogens on the other side.

The conformation where only one hydrogen is rotated is energetically more stable than the cis structure (see the 6-31G study by Nguyen et al.[43]), but my primary objective was to see if the anomalous intensities predicted by SCF theory for triimide would also arise in other triimide conformations. The symmetry of the cis structure made it the computationally attractive candidate. The intensities of the B_2 vibrational modes whose SCF-DZP frequencies are 1871, 1580, and 1413 are all found to be unreasonably large. Only one intensity calculated with the DZ basis set is erroneously large, but its value is over 1000 km/mol. Again I expect that the anomalous results are due to the shortcomings of the single-reference SCF description of a molecule with biradical character.

Hydrogen, Nitrogen, and Ammonia

Hydrogen, nitrogen, and ammonia were optimized using DZP basis sets at the SCF and MBPT(2) levels of theory. Also, vibrational

Table 5.12. Optimum Geometries and Electronic Energies of cis-Triimide

Bond or Angle	Bond Distances (Å) and Bond Angles in Degrees SCF Level of Theory Basis Set DZ	DZP
N1-N2	1.285	1.258
H4-N1	1.010	1.013
H5-N2	1.010	1.005
θ(N2N1N3)	123.58	125.25
θ(H4N1N2)	118.21	117.37
θ(H5N2N1)	109.76	107.37
Energy (a.u.)	-164.88322	-164.99448

a

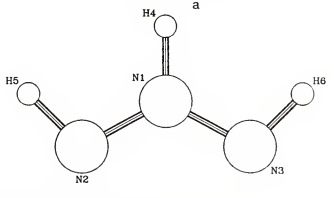

a) Molecule has C_{2v} symmetry.

Table 5.13. Vibrational Frequencies and Intensities of cis-Triimide

Vibrational Mode	Vibrational Frequencies (cm-1) SCF Level of Theory Basis Set DZ[a]	DZP[a]
A_1	3713 (0.926)	3765 (0.702)
B_2	3698 (13.6)	3754 (21.4)
A_1	3631 (10.1)	3634 (3.51)
B_2	1885 (66.4)	1871 (230.7)
A_1	1616 (4.86)	1689 (14.0)
B_2	1582 (171.9)	1580 (240.0)
A_1	1316 (0.550)	1369 (0.0004)
B_2	1286 (1088.4)	1413 (840.6)
B_1	1182 (24.2)	1153 (6.92)
B_1	860 (220.0)	863 (138.6)
A_1	713 (0.0250)	734 (0.511)
A_2[b]	627 (0.00)	670 (0.00)

a) Intensities are shown in parentheses in units of km/mole.

b) IR vibrational transition is forbidden by symmetry.

frequencies for these three molecules were computed at both levels. The results of these calculations are given in Table 5.14. The geometries of the known molecules are in fair agreement with experiment.[64,65,66] The experimental frequencies reported for H_2 and N_2 are actually experimental frequencies computed with a harmonic force field.[64] The DZP-MBPT(2) calculated frequencies for H_2 and N_2 still differ by 4.07% and 9.79%, respectively. The calculated values for N_2 are especially poor due to the difficulty in describing the triple bond. Note that the DZP-MBPT(2) value for the bond distance is off by 0.041 Å for N_2, yet within 0.003 Å for both H_2 and NH_3. The experimental frequencies reported for NH_3 are true experimental values.[67] The average error for the DZP-MBPT(2) frequencies for NH_3 is 9.2%. This error is slightly larger than is usually obtained at the MBPT(2) level using a DZP basis set.

Relative Energies and Thermochemical Quantities

Relative energies for molecules and molecular pairs on the N_3H_3 hypersurface calculated at various levels of theory using SCF-DZP optimum geometries are reported in Table 5.15. $\frac{3}{2}(N_2 + H_2)$ was chosen as the reference point for the relative energies so that it also could be chosen as the reference point for the relative enthalpies. By convention, elements in their standard states at 298 K and one atmosphere pressure have zero enthalpies. Note that correlation lowers the relative energies of all of the N_3H_3 isomers and increases the relative energies of all the molecular pairs. While

Table 5.14. Optimum Geometries, Electronic Energies, and Vibrational Frequencies of Hydrogen, Nitrogen, and Ammonia

Molecule	Bond Distances (Å), Bond Angles in Degrees, and Vibrational Frequencies (cm-1) Basis Set and Level of Theory		
	SCF (DZP)	MBPT(2) (DZP)	Experiment
H_2			
r(H-H)	0.736	0.740	0.740[a]
E(a.u.)	-1.13100	-1.15842	---
ν	4637	4574	4395 [a]
N_2			
r(N-N)	1.080	1.135	1.094[a]
E(a.u.)	-108.96046	-109.29786	---
ν	2720	2129	2360 [a]
NH_3			
r(N-H)	1.003	1.017	1.011[b]
Θ(HNH)	107.82	105.68	106.6 [c]
E(a.u.)	-56.20890	-56.41235	---
ν			
E	3847	3702	3444 [d]
A_1	3712	3551	3337
E	1797	1699	1627
A_1	1121	1124	950

a) Reference 64

b) Reference 65

c) Reference 66

d) Reference 67

Table 5.15. Relative Energies at SCF-DZP Optimum Geometries

Molecule or Molecular Pair	Relative Energies (kcal/mole) Level of Theory				
	SCF	MBPT(2)	SDTQ-MBPT(4)	CCSD	CCSD + T(CCSD)
$3/2(N_2+H_2)$[a]	0.0	0.0	0.0	0.0	0.0
N_2 + NH_3	-20.19	-18.15	-17.14	-18.62	-17.61
Triazene	49.54	47.32	46.13	45.17	44.45
Triimide	79.85	61.70	62.85	66.00	62.57
Triaziridine	94.45	88.77	88.20	86.64	86.49
cis-Triimide	89.55	71.57	72.54	75.18	71.73
cis-Triaziridine	105.78	99.38	98.41	96.98	96.62

a) The absolute energies (a.u.) for 3/2(nitrogen + hydrogen) are as follows: SCF -165.13718, MBPT(2) -165.67320, SDTQ-MBPT(4) -165.71257, CCSD -165.69348, CCSD+T(CCSD) -165.71054.

correlation stabilizes all of the N_3H_3 isomers relative to $\frac{3}{2}(N_2 + H_2)$, the relative energies of triimide and cis-triimide are lowered the most. This result is due to the coupled-cluster method attempting to recover the effects of the b_1 configuration. Contributions to the energy due to triple excitations are greatest for triimide and cis-triimide for the same reason. Certain triple excitations out of the a_2 configuration are equivalent to single excitations out of the b_1 configuration.

Relative energies for selected N_3H_3 isomers and molecular pairs calculated at MBPT(2) optimum geometries at various levels of theory are presented in Table 5.16. Relative energies at the highest level of theory employed, CCSD + T(CCSD), differ only slightly from corresponding values reported in Table 5.15; all are increased by 0.5 to 2.0 kcal/mol.

Table 5.17 lists the themochemical quantities computed from the ab initio results for the N_3H_3 isomers, hydrogen, nitrogen, and ammonia. Comparison of the Gibbs free energies of the different systems with the electronic relative energies reported in Tables 5.15 and 5.16 reveals that $\frac{3}{2}(N_2 + H_2)$ is stabilized relative to $N_2 + NH_3$, but that all of the N_3H_3 isomers are less stable than the electronic energies alone report. Obvoiusly, the synthesis and isolation of any of the N_3H_3 molecules poses quite a difficult experimental task. Transition states and corresponding barrier heights will need to be determined in future work in order to have some idea of how long-lived any of these species might be to determine if they may be isolated.

Table 5.16. Relative Energies at the MBPT(2)-DZP Optimum Geometries

Molecule or Molecular Pair	Relative Energies (kcal/mole) Level of Theory					
	SCF	MBPT(2)	SDQ-MBPT(4)	SDTQ-MBPT(4)	CCSD	CCSD + T(CCSD)
$3/2(N_2+H_2)$[b]	0.0	0.0	0.0	0.0	0.0	0.0
$N_2 + NH_3$	-22.72	-16.18	-17.86	-15.59	-18.12	-16.61
Triazene	44.36	51.35	47.21	48.99	45.95	45.95
Triimide	75.59	64.83	67.22	64.63	66.53	63.25
Triaziridine	89.91	92.31	88.42	90.42	86.79	87.19

[a] The absolute energies (a.u.) for 3/2(nitrogen + hydrogen) are as follows: SCF -165.12316, MBPT(2) -165.68442, SDQ-MBPT(4) -165.69983, SDTQ-MBPT(4) -165.72228, CCSD -165.69796, CCSD+T(CCSD) -165.71776.

Table 5.17. Thermodynamic Variables Computed at the SCF-DZP and MBPT(2)-DZP Levels of Theory

Molecule or Molecular Pair	Thermodynamic Variables at 298 K and One Atmosphere of Pressure				
	Zero-point[a] Energy	Enthalpy[a,b]	Entropy[c]	Gibbs[a] Free Energy	Heat[c] Capacity (const. V)
$3/2(N_2+H_2)$					
SCF	15.78	0.0	115.18	-34.34	14.90
MBPT(2)	14.37	0.0	115.51	-34.44	14.91
$N_2 + NH_3$					
SCF	26.94	-10.79	91.57	-38.09	11.24
MBPT(2)	25.17	-7.15	91.85	-34.53	11.27
Triazene					
SCF	31.74	61.97	59.64	44.19	9.56
MBPT(2)	29.40	62.89	60.03	44.99	10.07
Triimide					
SCF	32.45	92.84	57.65	75.65	8.39
MBPT(2)	30.02	76.88	58.17	59.53	9.19
Triaziridine					
SCF	32.90	107.81	58.55	90.36	7.57
MBPT(2)	29.90	104.15	59.07	86.54	8.55
cis-Triimide					
SCF	32.16	102.28	57.66	85.09	8.74
cis-Triaziridine					
SCF	32.47	118.72	56.43	101.90	7.69

[a] Values are given in kcal/mol.

[b] Enthalpies have been adjusted so that elements in their standard states have enthalpies of zero at 298 K and 1 atm of pressure.

[c] Values are given in cal/(mol * °K).

Vibrational Spectra

One may simulate an experimental matrix-isolated spectrum by using a sum of Lorentzian linefunctions. The absorbance Y_i for each frequency point x_i is calculated as

$$Y_i(x_i) = \frac{1}{\pi} \sum_j \frac{S_j \Delta_j}{(x_i - \omega_j)^2 + \Delta_j^2}$$

where S_j represents the integrated absorbance of each band; Δ_j, the half bandwidth at half of the maximum absorbance; and ω_j, the frequency of the band center. The integrated absorbance is equal to the product of the calculated intensity, the path length, and the concentration, but these latter two variables are set to unity. The calculated frequencies are the frequencies of the band centers. For these unknown molecular systems, I use 2.5 wavenumbers for the half bandwidth of all peaks. This value is probably somewhat small for many of the peaks, but should be a reasonable average value. The infrared spectra for triaziridine, triimide, and triazene are plotted in Figures 5.1-5.6 using the computed MBPT(2)-DZP and SCF-DZP frequencies and intensities. Note that E(2) denotes MBPT(2) in these figures. The SCF infrared spectra for the cis isomers are presented in Figures 5.7 and 5.8. In all eight spectra, the largest absorption is normalized to the same absorption value. This normalization is made to help the calculated spectra more closely resemble an experimental spectrum and is equivalent to changing the path length and concentration for each system.

In comparing the SCF-DZP infrared spectrum of triaziridine in Figure 5.1 with the corresponding MBPT(2)-DZP spectrum in Figure 5.2,

the importance of correlation is evident. Not only are the band centers shifted to lower frequencies as expected, but the relative intensities and the grouping of the peaks are different. The two spectra cannot be made to coincide by simply scaling the SCF values. In Figures 5.3 and 5.4, the difference in the SCF and MBPT(2) spectra of triimide is exaggerated due to the large anomalous SCF intensity of 839 km/mole. However, changes in relative peak heights may still be observed.

The two spectra of triazene in Figures 5.5 and 5.6 perhaps provide the best correspondence between the two levels of theory. At the MBPT(2) level the frequencies of the band centers are lower and the relative intensities of the stronger bands between 1000 and 2000 wavenumbers have leveled out to approximately the same peak height. Other than this, there appears to be little difference. However, recall that the order of two of the bands has shifted in the MBPT(2) results from the SCF order.

The SCF-DZP spectra for the two cis isomers are presented in Figures 5.7 and 5.8. The D_{3h} symmetry of cis-triaziridine causes many of the frequencies of its normal modes to be degenerate. This degeneracy is easily observed in the spectrum by the relatively few distinct band centers. As with triimide, the accuracy of the SCF spectrum for cis-triimide is diminished by the large anomalous intensities.

Figure 5.1 Triaziridine SCF IR Spectrum

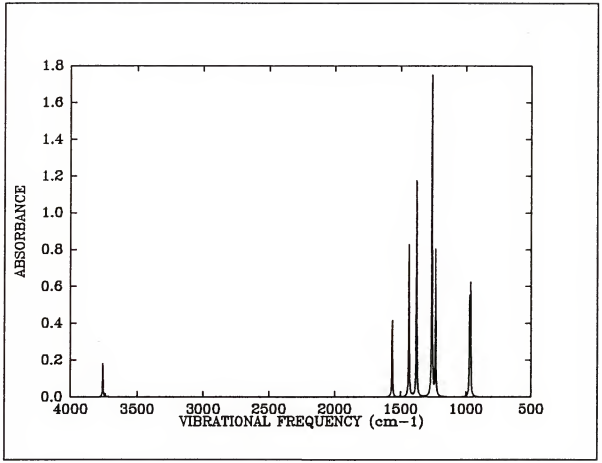
ABSORBANCE
1.8
1.6
1.4
1.2
1.0
0.8
0.6
0.4
0.2
0.0
4000
3500
3000
2500
2000
1500
1000
500
VIBRATIONAL FREQUENCY (cm-1)

Figure 5.2 Triaziridine E(2) IR Spectrum

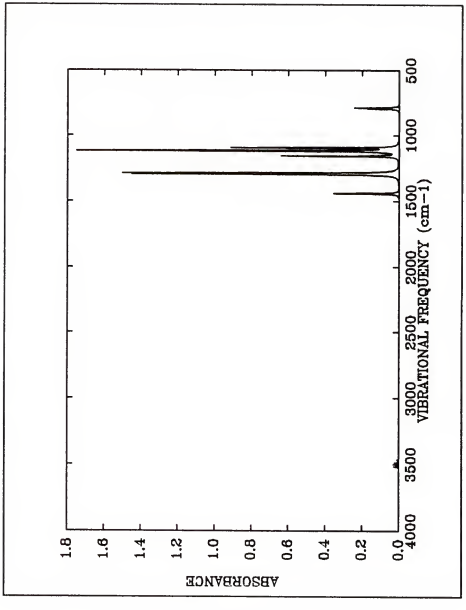
ABSORBANCE
1.8
1.6
1.4
1.2
1.0
0.8
0.6
0.4
0.2
0.0
4000
3500
3000
2500
2000
1500
1000
500
VIBRATIONAL FREQUENCY (cm-1)

Figure 5.3 Triimide SCF IR Spectrum

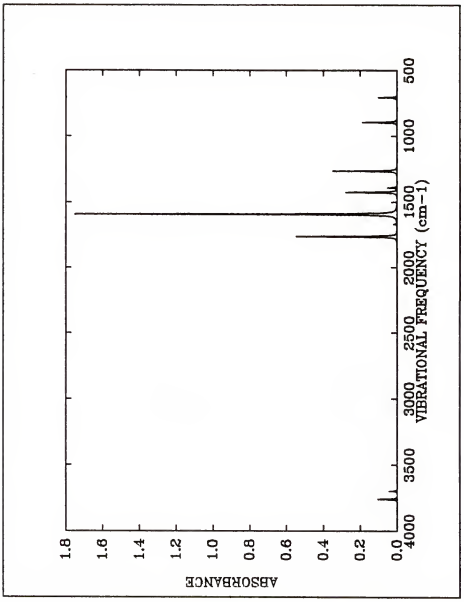
ABSORBANCE
1.8
1.6
1.4
1.2
1.0
0.8
0.6
0.4
0.2
0.0
4000
3500
3000
2500
2000
1500
1000
500
VIBRATIONAL FREQUENCY (cm-1)

Figure 5.4 Triimide E(2) IR Spectrum

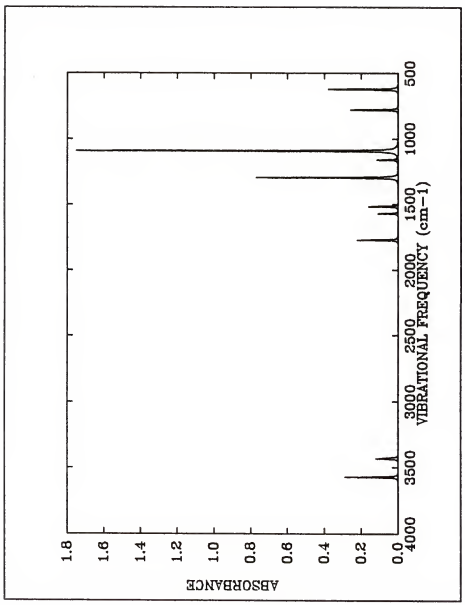
ABSORBANCE
1.8
1.6
1.4
1.2
1.0
0.8
0.6
0.4
0.2
0.0
4000
3500
3000
2500
2000
1500
1000
500
VIBRATIONAL FREQUENCY (cm-1)

Figure 5.5 Triazene SCF IR Spectrum

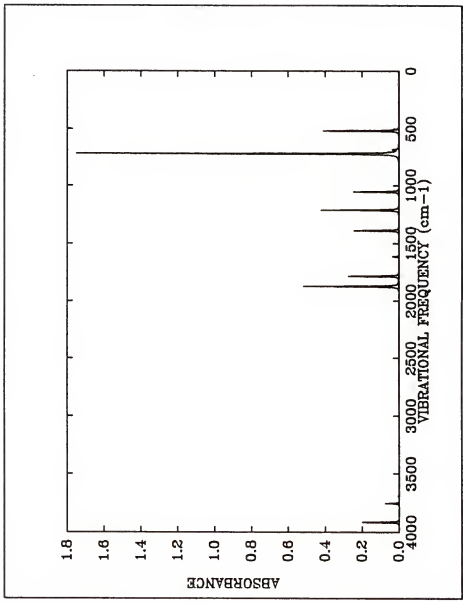
ABSORBANCE
1.8
1.6
1.4
1.2
1.0
0.8
0.6
0.4
0.2
0.0
4000
3500
3000
2500
2000
1500
1000
500
0
VIBRATIONAL FREQUENCY (cm-1)

Figure 5.6 Triazene E(2) IR Spectrum

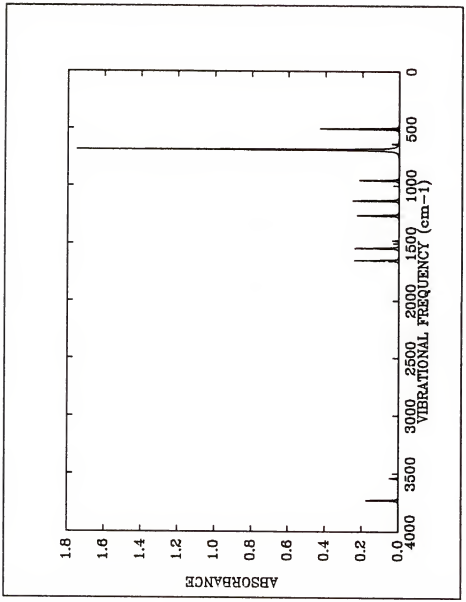
ABSORBANCE
1.8
1.6
1.4
1.2
1.0
0.8
0.6
0.4
0.2
0.0
4000
3500
3000
2500
2000
1500
1000
500
0
VIBRATIONAL FREQUENCY (cm-1)

Figure 5.7 Cis-Triaziridine SCF IR Spectrum

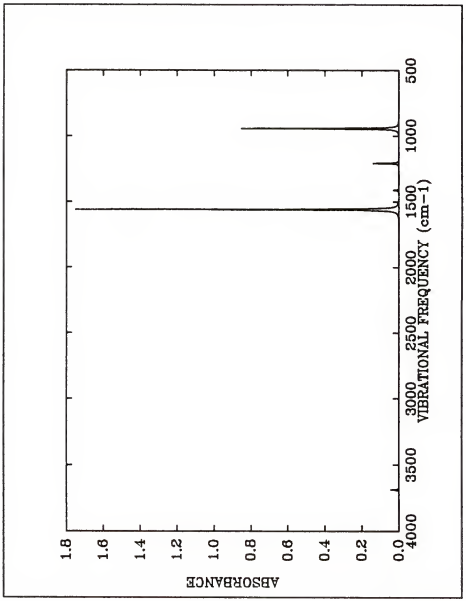
ABSORBANCE
1.8
1.6
1.4
1.2
1.0
0.8
0.6
0.4
0.2
0.0
4000
3500
3000
2500
2000
1500
1000
500
VIBRATIONAL FREQUENCY (cm-1)

Figure 5.8 Cis-Triimide SCF IR Spectrum

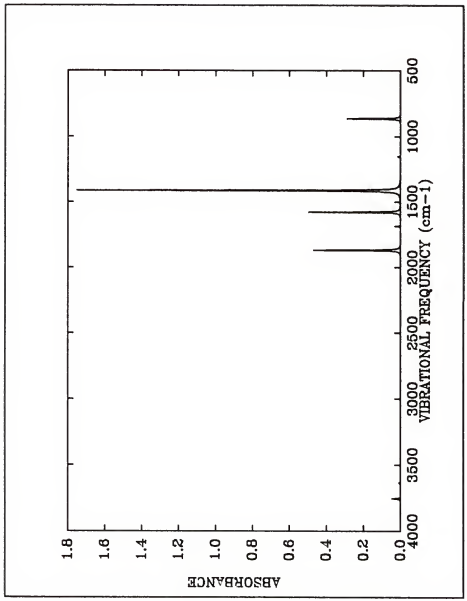
ABSORBANCE
1.8
1.6
1.4
1.2
1.0
0.8
0.6
0.4
0.2
0.0
4000
3500
3000
2500
2000
1500
1000
500
VIBRATIONAL FREQUENCY (cm-1)

CHAPTER 6
A COUPLED-CLUSTER EFFECTIVE HAMILTONIAN FOR EXCITATION ENERGIES

Consider an excitation operator Ω_k which takes the electronic ground state wavefunction into the kth excited state:

$$\Omega_k \Psi_0 = \Psi_k \ . \tag{6.1}$$

If $H\Psi_0 = E_0\Psi_0$ and $H\Psi_k = E_k\Psi_k$, then $H\Omega_k\Psi_0 = H\Psi_k = E_k\Psi_k = E_k\Omega_k\Psi_0$ and $\Omega_k H\Psi_0 = \Omega_k E_0\Psi_0 = E_0\Omega_k\Psi_0$. From the difference of these latter two equations, the equation of motion governing the excitation operator and the excitation energy (ω_k) is obtained:

$$([H,\Omega_k])\Psi_0 = (E_k - E_0)\Omega_k\Psi_0 = \omega_k\Omega_k\Psi_0 \ .^{68\text{-}72} \tag{6.2}$$

From this equation different methods for calculating electronic excitation energies may be formulated by the choices of Ψ_0 and Ω_k. For example, if the SCF reference function Φ is chosen to describe Ψ_0 and the excited state operator is represented by some linear combination of single particle excitations such as

$$\Omega_k = \sum_{i,a} S_{ia}(k)\ a^+ i \ ,$$

then we have the Tamm-Dancoff approximation.

Here, I begin by choosing Ψ_0 to be represented by the coupled-cluster wavefunction, $e^T|0\rangle$, where $|0\rangle$ is some single determinant reference function. Thus Equation 6.2 becomes

$$[H,\Omega_k]e^T|0\rangle = \omega_k\Omega_k e^T|0\rangle \quad .^{69-72} \tag{6.3}$$

In the formulation of ordinary coupled-cluster theory outlined in the second chapter, the Hamiltonian was replaced by H_N to aid in the derivation of the energy and t-amplitude equations. Can the same substitution be made in Equation 6.3? Recall that $H_N = H - \langle 0|H|0\rangle$ and consider the following:

$$\begin{aligned}
[H,\Omega_k]e^T|0\rangle &= H\Omega_k e^T|0\rangle - \Omega_k H e^T|0\rangle \\
&= H\Omega_k e^T|0\rangle - \langle 0|H|0\rangle\ \Omega_k e^T|0\rangle - \\
&\qquad \Omega_k H e^T|0\rangle + \langle 0|H|0\rangle\ \Omega_k e^T|0\rangle \\
&= H\Omega_k e^T|0\rangle - \langle 0|H|0\rangle\ \Omega_k e^T|0\rangle - \\
&\qquad \left[\Omega_k H e^T|0\rangle - \Omega_k\langle 0|H|0\rangle\ e^T|0\rangle\right] \\
&= H_N\Omega_k e^T|0\rangle - \Omega_k H_N e^T|0\rangle \\
&= \left[H_N,\Omega_k\right] e^T|0\rangle \quad .
\end{aligned}$$

Thus,

$$[H_N,\Omega_k]\ e^T|0\rangle = \omega_k\Omega_k e^T|0\rangle \quad . \tag{6.4}$$

Also note that since $He^T|0\rangle = E_0 e^T|0\rangle$ and $H\Omega_k e^T|0\rangle = E_k\Omega_k e^T|0\rangle$, it follows from the above derivation that $H_N e^T|0\rangle = \Delta E_0 e^T|0\rangle$ and $H_N\Omega_k e^T|0\rangle = \Delta E_k e^T|0\rangle$ where $\Delta E_k = E_k - \langle 0|H|0\rangle$. Therefore, $\omega_k = E_k - E_0 = \Delta E_k - \Delta E_0$. The excitation energy ω_k is both the difference between the total energies of the two states and the difference

between the correlation energy of the ground state and the correlation-like energy of the excited state.

Now, without making a specific choice of $\mathfrak{Q}_k$, let me place the restriction on $\mathfrak{Q}_k$ to be of the same form as T so that $[\mathfrak{Q}_k, e^T] = 0$. Thus Equation 6.4 becomes

$$\left(H_N e^T \mathfrak{Q}_k\right)|0\rangle - \mathfrak{Q}_k H_N e^T|0\rangle = \omega_k e^T \mathfrak{Q}_k|0\rangle \ . \tag{6.5}$$

Projection on the left by e^{-T} then yields

$$e^{-T}H_N e^T \mathfrak{Q}_k|0\rangle - \mathfrak{Q}_k e^{-T}H_N e^T|0\rangle = \omega_k \mathfrak{Q}_k|0\rangle \ . \tag{6.6}$$

From ordinary coupled-cluster theory, we know that $e^{-T}H_N e^T = (H_N e^T)_c$. Therefore, let me define $(H_N e^T)_c = \bar{H}_N$ to be an effective Hamiltonian so that Equation 6.6 becomes

$$[\bar{H}_N, \mathfrak{Q}_k]|0\rangle = \omega_k \mathfrak{Q}_k|0\rangle. \tag{6.7}$$

Unlike the ordinary normal-ordered Hamiltonian which is limited to one-body and two-body parts, the effective Hamiltonian has no such restrictions:

$$\bar{H}_N = \bar{F}_N + \bar{V}_N + III_N + IV_N + \ldots \tag{6.8}$$

where III_N = three-body terms, IV_N = four-body terms, etc. However, for a truncation of T, the number of terms for $\bar{H}_N$ will terminate. These individual components of $\bar{H}_N$ are sums of terms which involve contractions of the ordinary normal-ordered Hamiltonian and the e^T operators. Thus, these components may be constructed and represented diagrammatically by using the operator diagrams of H_N and T_1, T_2, ... The operator diagrams for H_N were presented in Figure 2.1, and for the

CCSDT model the diagrams representing T_1, T_2, and T_3 were presented in Figures 2.4, 2.5, and 2.6, respectively.

The diagrammatic equations for $\bar{F}_N$, $\bar{V}_N$, and III_N in the CCSDT model are given in Figures 6.1, 6.2, and 6.3, respectively. Note that an n-body term of $\bar{H}_N$ has $(n + 1)^2$ components. For example, $\bar{F}_N$ has four terms just like f_N in the ordinary normal-ordered Hamiltonain, and $\bar{V}_N$ has nine components just like V_N. III_N has 16 component terms, but notice that not all of these have any contributions from the possible contractions of H_N and e^T. Specifically, there are no contributing diagrams to diagrams A through G and diagram J in Figure 6.3. The reason these terms have no contributions is easy to see. Each of these diagrams require either three particle or three hole lines at the bottom of the diagram (below the vertex of the diagram). The T operators are restricted to be excitation operators; they have no unconnected lines below the vertex. H_N can have four unconnected lines below the vertex, but never more than two particle and two hole lines. Thus, it is impossible to get a contraction from H_N and e^T that yields a diagram having three particle or three hole lines below the vertex.

Comparison of the 37 diagrams which contribute to diagram I of Figure 6.2 with the 37 diagrams which contribute to T_2 in the CCSDT equations given in Figure 2.5 reveals that they are the same. Thus for the CCD model, all amplitudes of diagram I in Figure 6.2 are zero when the converged t_2 amplitudes are used to construct $\bar{V}_N$ due to the defining equation of the t_2 amplitudes:

$$\langle D|(H_N e^T)_C|0\rangle = 0$$

where D is a doubly excited determinant. Similarly, all amplitudes corresponding to diagram D of Figure 6.1, as well as those corresponding to diagram I of Figure 6.2, are zero in the CCSD model and these amplitudes plus those amplitudes corresponding to diagram P of Figure 6.3 are zero when the CCSDT model is used in the ordinary coupled-cluster calculation.

Because $\bar{H}_N$ comprises all contracted products of H_N and e^T, there actually is one other component to $\bar{H}_N$ that is not listed in Equation 6.8, namely the zero-body term or fully-contracted products of H_N and e^T. The diagrammatic representation of this zero-body term is simply the diagrammatic representation of the CC energy expression which was presented in Figure 2.3. Thus, this zero-body term is a constant, the correlation energy of the ground state. (ΔE_0).

Consider how this zero-body term affects the equation of motion. Let $\bar{H}_N$ of Equation 6.7 be denoted by $\bar{H}_N(Z)$ to distinguish it from the $\bar{H}_N$ of Equation 6.8 which no longer contains the zero-body component. By inserting $\hat{1} = |P><P|$ into Equation 6.7, we obtain

$$\bar{H}_N(Z)|P><P|\Omega_k|0> - |P><P|\Omega_k\bar{H}_N(Z)|0> = \omega_k|P><P|\Omega_k|0> \qquad (6.9)$$

where $|P>$ represents the sum of all possible excited determinants formed from the chosen reference function plus the reference function itself. Now, recall that $\bar{H}_N|0> = (H_N e^T)_c|0> = \Delta E_0|0>$. Equation 6.9 becomes

$$\begin{aligned}\omega_k|P><P|\Omega_k|0> &= \bar{H}_N(Z)|P><P|\Omega_k|0> - |P><P|\Omega_k\Delta E_0|0> \\ &= (\bar{H}_N(Z) - \Delta E_0)|P><P|\Omega_k|0> \qquad (6.10)\end{aligned}$$

$$= \bar{H}_N|P\rangle\langle P|\Omega_k|0\rangle$$

where $\bar{H}_N$ in the last line of the above expression is the $\bar{H}_N$ of Equation 6.8 where the zero-body term has been removed. The second term arising from the commutator in the equation of motion merely serves to remove the zero-body term from $\bar{H}_N(Z)$ to produce $\bar{H}_N$.

Now project on the left of Equation 6.10 with $\langle P|$ to obtain

$$\langle P|\bar{H}_N|P\rangle\langle P|\Omega_k|0\rangle = \omega_k\langle P|\Omega_k|0\rangle \qquad (6.11)$$

and choose Ω_k to be the excitation operator which takes the reference function into singly and doubly excited determinants:

$$\Omega_k = \sum_{i,a} S_i^a\, a^+i \;+\; \sum_{\substack{i,j,\\ a,b}} S_{ij}^{ab}\, a^+ib^+j \quad .$$

If the reference function is the SCF ground-state wavefunction (or any determinant formed from an orthonormal set of orbitals), then all excited determinants form an orthonormal set:

$$\langle D_i^a \mid D_j^b \rangle = \delta_{ab}\delta_{ij}$$

$$\langle D_i^a \mid D_{jk}^{bc} \rangle = 0$$

etc.

Therefore, with the above choice of Ω_k, $\langle P|\Omega_k|0\rangle = 0$ for $\langle P|$ = triply excited determinants and higher.

Equation 6.11 can now be viewed as being analogous to a CISD matrix eigenvalue equation. By considering all possible k excited states which can be formed from our choice of Ω_k, we have a matrix

comprising all single and double excitations. However, this matrix is very different from the ordinary CISD matrix. It is the matrix representation of the effective Hamiltonian with eigenvalues that are excitation energies rather than the total electronic energies of the excited states. Since the relevant matrix elements are of the form $\Omega_k^+ \bar{H}_N \Omega_k$, we have a single-single block, a single-double block, a double-single block, and a double-double block. Thus, only the terms of III_N represented by diagrams H, I, and L in Figure 6.3 can contribute to the equations of the matrix elements, and any term of $\bar{H}_N$ beyond III_N cannot contribute at all.

Unlike the ordinary CISD matrix, the matrix representation of $\bar{H}_N$ is non-Hermitian. The single-double block of the matrix ($\langle S|\bar{H}_N|D\rangle$) is different from the double-single block. In particular, note that the single-double block will involve contributions from matrix elements from $\bar{f}_N$ which arise from contractions with diagram A of Figure 6.1, but the double-single block will not have corresponding contributions from $\bar{f}_N$. The only possible fully-contracted terms would involve amplitudes from Diagram D in Figure 6.1, and these amplitudes are all zero for the converged CCSD equations.

One other major difference exists between the effective Hamiltonian matrix and an ordinary CISD matrix. In an ordinary CISD calculation relative to an SCF reference function, the doubly excited determinants correlate the ground state, and the singly excited determinants affect the ground-state only indirectly by mixing with the doubles. In the effective Hamiltonian matrix, neither the single-single block nor the double-double block mix with the CC ground state

as long as T contains both T_1 and T_2. $\langle S|\bar{H}_N|0\rangle = 0$ and $\langle D|\bar{H}_N|0\rangle = 0$ are the defining equations of the t_1 and t_2 amplitudes in CCSD theory.

Now that the theory of the coupled-cluster effective Hamiltonian for excitation energies has been developed, the reliability of the method needs to be tested. Therefore, results from an initial implementation of the theory are presented in the next chapter.

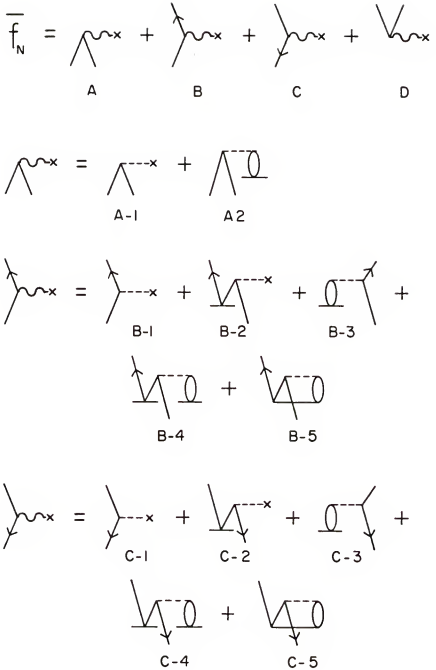

Figure 6.1. The Diagrammatic Representation of $\bar{f}_N$ in the CCSDT Model.

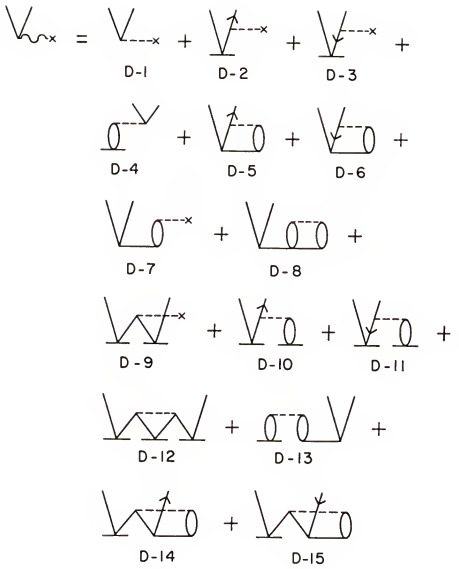

Figure 6.1--continued

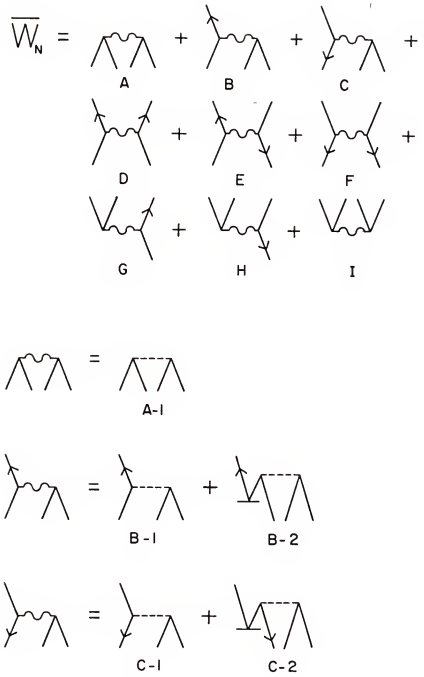

Figure 6.2. The Diagrammatic Representation of $\overline{V}_N$ in the CCSDT Model.

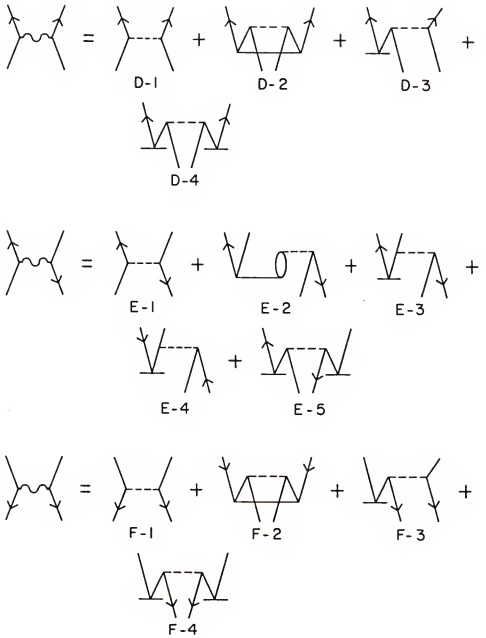

Figure 6.2--continued

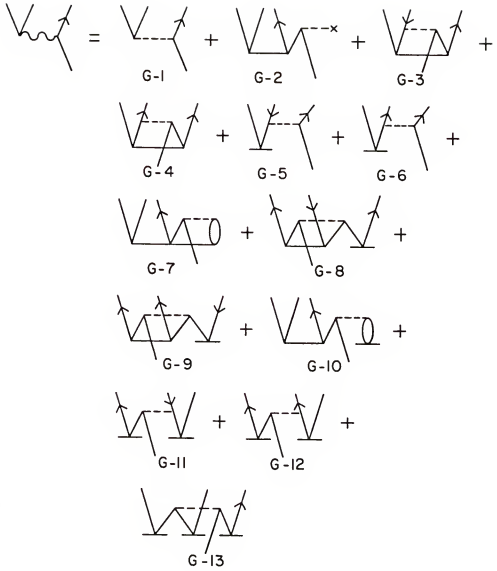

Figure 6.2--continued

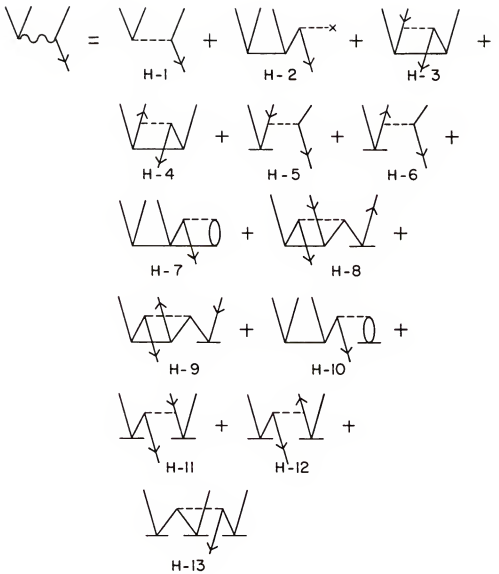

Figure 6.2--continued

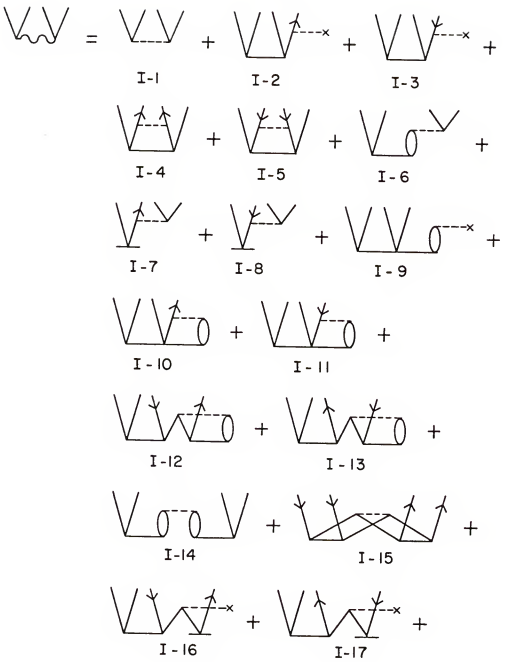

Figure 6.2--continued

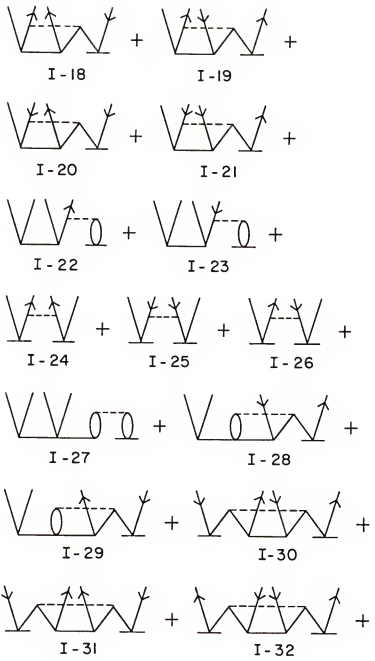

Figure 6.2--continued

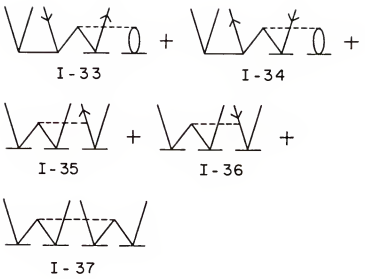

Figure 6.2--continued

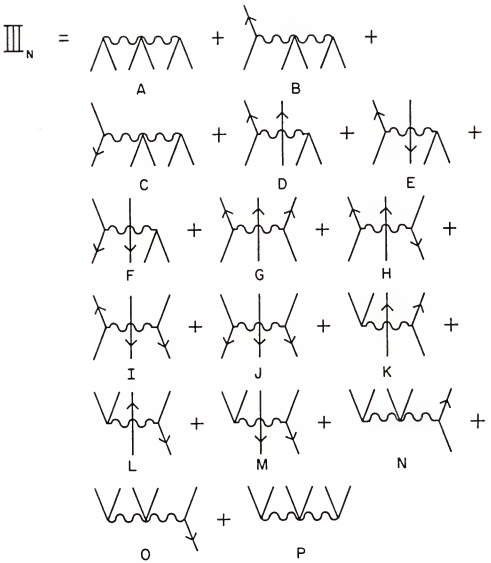

Figure 6.3. The Diagrammatic Representation of III_N in the CCSDT Model.

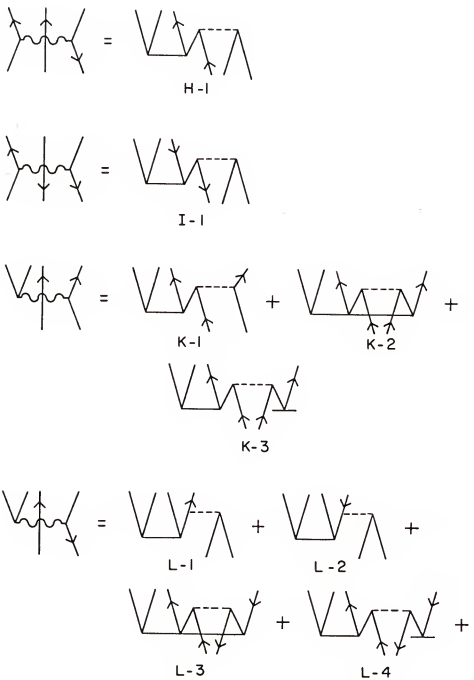

Figure 6.3--continued

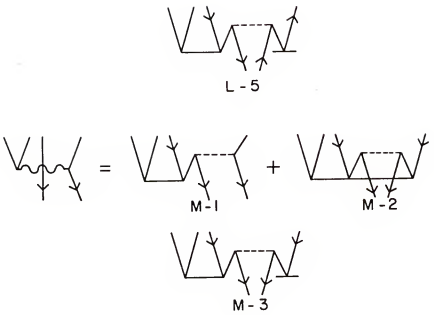

Figure 6.3--continued

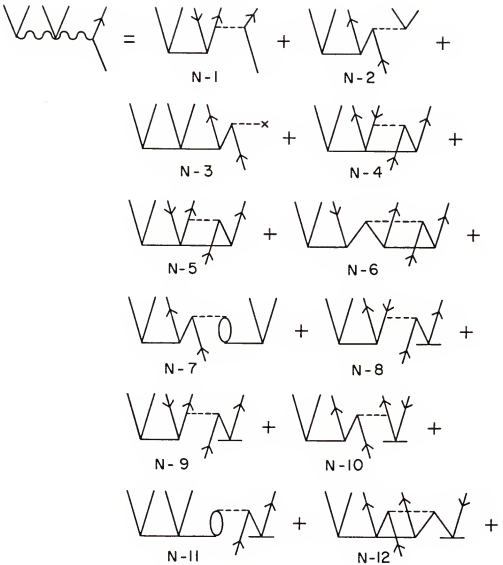

Figure 6.3--continued

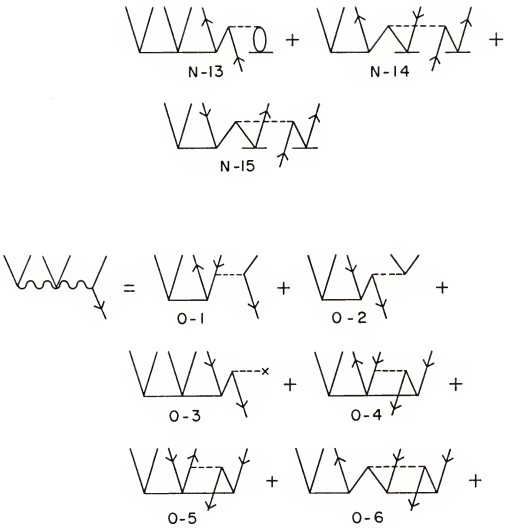

Figure 6.3--continued

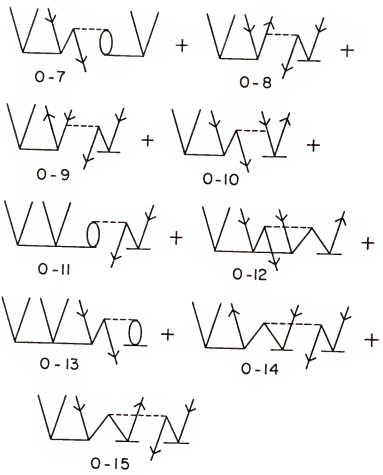

Figure 6.3--continued

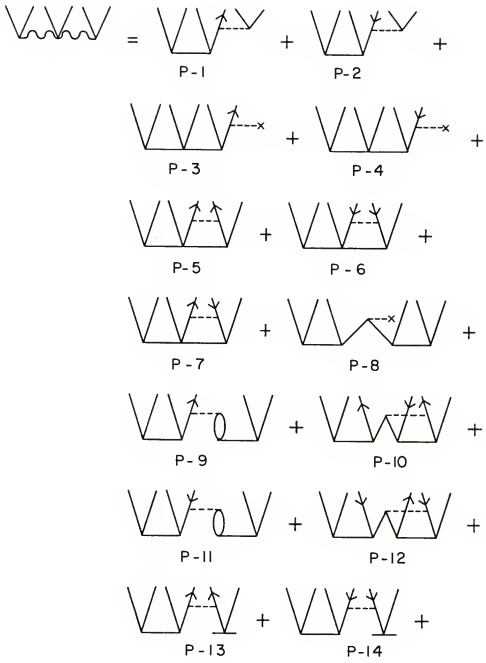

Figure 6.3--continued

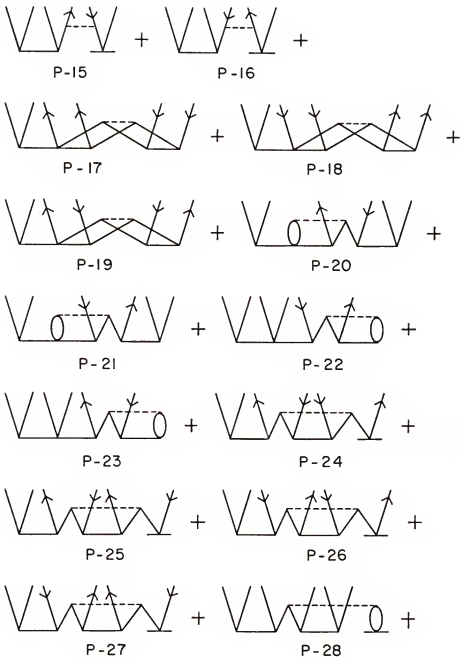

Figure 6.3--continued

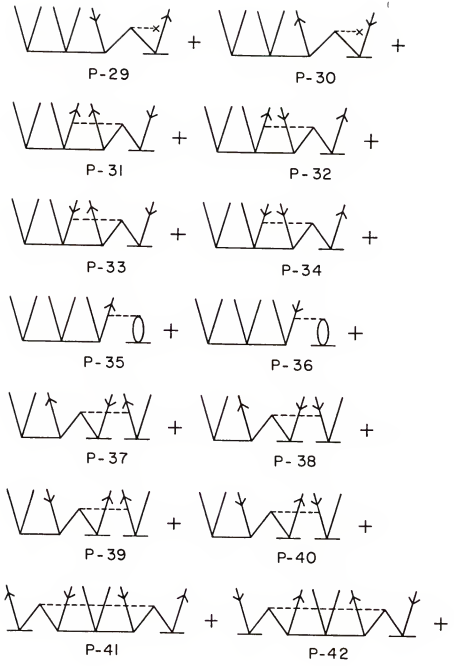

Figure 6.3--continued

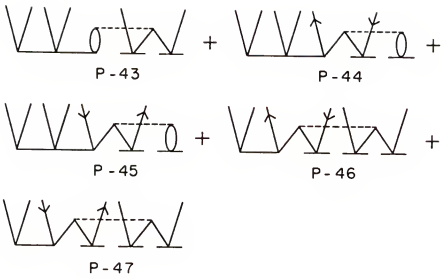

Figure 6.3--continued

CHAPTER 7
EXCITATION ENERGY RESULTS AND DISCUSSIONS

Let $\bar{H}_N(SS)$ denote the single-single block of the matrix representation of the normal-ordered effective Hamiltonian. Similarly, let $\bar{H}_N(SD)$ denote the single-double block, $\bar{H}_N(DS)$ denote the double-single block, and $\bar{H}_N(DD)$ denote the double-double block. The spin-adapted equations used to compute the matrix elements of $\bar{H}_N$ are

$$\bar{H}_N(SS)_{ia,jb} = \langle a|\bar{f}_N|b\rangle\delta_{ij} - \langle j|\bar{f}_N|i\rangle + [1 + (-1)^S]\langle aj|\bar{v}_N|ib\rangle - \langle aj|\bar{v}_N|bi\rangle ,$$

$$\bar{H}_N(SD)_{ia,klcd} = [1 + (-1)^S]\langle l|\bar{f}_N|d\rangle\delta_{ac}\delta_{ik} - \langle l|\bar{f}_N|c\rangle\delta_{ad}\delta_{ik} + [1 + (-1)^S]\left(\langle al|\bar{v}_N|cd\rangle\delta_{ik} - \langle kl|\bar{v}_N|id\rangle\delta_{ac}\right) + \langle lk|\bar{v}_N|id\rangle\delta_{ac} - \langle al|\bar{v}_N|dc\rangle\delta_{ik} ,$$

$$\bar{H}_N(DS)_{mnef,jb} = \langle jf|\bar{v}_N|nm\rangle\delta_{eb} - \langle fe|\bar{v}_N|bn\rangle\delta_{jm} + [1 + (-1)^S]\left(\langle ef|\bar{v}_N|bn\rangle\delta_{jm} - \langle jf|\bar{v}_N|mn\rangle\delta_{be}\right) ,$$

$$\bar{H}_N(DD)_{mnef,klcd} = \langle f|\bar{f}_N|c\rangle\delta_{nk}\delta_{ed}\delta_{lm} + \langle e|\bar{f}_N|c\rangle\delta_{mk}\delta_{df}\delta_{ln} -$$

$$\langle k|\bar{F}_N|n\rangle\delta_{fc}\delta_{ml}\delta_{ed} - \langle k|\bar{F}_N|m\rangle\delta_{ec}\delta_{nl}\delta_{fd} +$$

$$[1 + (-1)^S]\left(\langle fk|\bar{V}_N|nc\rangle\delta_{ed}\delta_{lm} + \langle ek|\bar{V}_N|mc\rangle\delta_{fd}\delta_{ln}\right)$$

$$- \langle fk|\bar{V}_N|cn\rangle\delta_{ed}\delta_{lm} + \langle ek|\bar{V}_N|cm\rangle\delta_{fd}\delta_{ln} -$$

$$\langle ek|\bar{V}_N|md\rangle\delta_{ln}\delta_{fc} - \langle fk|\bar{V}_N|nd\rangle\delta_{lm}\delta_{ec} -$$

$$\langle ek|\bar{V}_N|dn\rangle\delta_{fc}\delta_{lm} + \langle fk|\bar{V}_N|dm\rangle\delta_{ec}\delta_{ln} +$$

$$\langle ef|\bar{V}_N|cd\rangle\delta_{km}\delta_{ln} + \langle kl|\bar{V}_N|mn\rangle\delta_{ec}\delta_{fd}$$

where the s superscript is zero for singlet excitations and one for triplet excitations. Mukherjee and Mukherjee derived these formulas[70] using a nonorthogonal spin-adaptation scheme for the matrix representation of the effective Hamiltonian discussed in the previous chapter. Note that there are no matrix elements for $\bar{F}_N$ in the double-single block.

To achieve an initial implementation of the present method, the computation of $\bar{H}_N(DD)$ is limited to the diagonal elements. These elements are then "folded" into the single-single block via the partitioning technique[73] to give the relation

$$\left(\bar{H}_N(SS)'\right)_{pq} = \left(\bar{H}_N(SS)\right)_{pq} + \sum_r \frac{(\bar{H}_N(SD))_{pr} * (\bar{H}_N(DS))_{rq}}{(\bar{H}_N(SS))_{pp} - (\bar{H}_N(DD))_{rr}} \quad .$$

where $\bar{H}_N(SS)'$ is the new matrix to be diagonalized. It is the size of the TDA matrix, yet represents a low-order partitioning of the full EOM-CCSD matrix which comprises all single and double excitations.

Vertical excitation energies for N_2 obtained with the above equations and with the approximation just given are presented in Table 7.1. They are compared to results obtained from a Fock matrix multi-reference coupled-cluster (MRCC) method for excitation energies.[74] The MRCC method differs from that used here primarily in that an exponential wavefunction is employed for each excited state.

Note that TDA-like excitation energies are reported for $\bar{H}_N$ as well as the results obtained from the partitioning of the full singles and doubles EOM-CCSD matrix, but are much too high in all cases. The double-double block is needed to shift the excitation energies down into the range of experiment. This result is not surprising when one considers how the double-double block in an ordinary CISD matrix affects the ordinary TDA excitation energies. TDA excitation energies suffer from a lack of accuracy, but they are often within an eV or two of the experimental results.[20] When doubly excited determinants are allowed to mix with the singles, the resulting excitation energies are usually too low. Of course, this is assuming that the CISD excitation energies are taken directly from the diagonalized matrix where the SCF energy is the reference energy. If the excitation energies are calculated from the CISD matrix with the correlated energy for the ground state, the excitation energies will usually be too high since the reference state is usually better correlated than any of the excited states. While this latter method is preferred if one actually wanted to use an ordinary CISD matrix to calculate excitation energies, the former is more closely related to the effective Hamiltonian where the ground state energy is not changed by the matrix diagonalization.

Table 7.1 Vertical Excitation Energies of Nitrogen

Excited State	Vertical Excitation Energies (eV) Level of Theory					
	TDA	RPA	MRCC[a]	$\bar{H}_N(SS)$[b]	$\bar{H}_N$[b,c]	EXP.[d]
$^3\Sigma_u^+$	6.03	2.58	7.73	8.51	7.31	7.8
$^3\Pi_g$	7.51	7.24	7.66	9.83	7.48	8.1
$^3\Delta_u$	7.24	5.85	9.33	10.24	8.68	8.9
$^1\Pi_g$	9.33	9.08	8.68	11.66	7.87	9.3
$^3\Sigma_u^-$	8.31	7.61	10.08	11.47	9.90	9.7
$^1\Sigma_u^-$	8.31	7.61	10.65	11.60	9.86	9.9
$^1\Delta_u$	8.99	8.65	10.99	12.35	10.43	10.3
$^1\Sigma_u^+$	17.21	15.59	17.14	18.49	15.26	14.4

a) Reference 74.

b) The effective Hamiltonian is calculated using the CCSD model.

c) Results are obtained from the partitioning of the EOM-CCSD matrix which comprises all singly and doubly excited determinants.

d) Reference 75.

Note All calculations for this table were performed with the standard DZ basis set.

Even with just the approximate inclusion of the double-double block, the CISD-like vertical excitation energies for $\bar{H}_N$ are in good agreement with the experimental results for nitrogen relative to the other theoretical methods. For example, the energy order of the $^3\Sigma_u^+$ and the $^3\Delta_u$ states is incorrect at both the TDA and RPA levels of theory., but correct in the effective Hamiltonian results. The $\bar{H}_N$ results are even better than the MRCC results for most states. It should be pointed out that the MRCC calculation was limited to the CCD model for $\bar{H}_N$, but this should make little difference. Even though the current approach should be done with the CCSD model to ensure that the single-single block does not mix with the ground state, we can force this restriction and use a CCD effective Hamiltonian anyway. Excitation energies for nitrogen calculated in this manner ($\bar{H}_N$ in the CCD model) differ very little from the CCSD $\bar{H}_N$ results (less than 0.05 eV for all states).

Vertical excitation energies for the beryllium atom are reported in Table 7.2. Here, the effective Hamiltonian results are compared to RPA excitation energies calculated using an antisymmetrized geminal powers (AGP)[76] reference function. Once again, the EOM-CCSD excitation energies for $\bar{H}_N$ obtained with the partitioning technique are better than the TDA and RPA results calculated from the SCF reference, but the AGP RPA results are closer to the experimental values for most states. It would appear that additional terms, such as the off-diagonal elements of the double-double block which are excluded in the partitioning technique, are needed to describe the electronic spectrum of beryllium well. Such terms are introduced into the AGP based RPA calculation.

Table 7.2 Vertical Excitation Energies of Beryllium

Excited State	Vertical Excitation Energies (eV) Level of Theory HF TDA	HF RPA	AGP[a] RPA	$\bar{H}_N(SS)$[b]	$\bar{H}_N$[b,c]	EXP.[d]
^3P	1.70	****[e]	2.74	2.94	2.30	2.73
^1P	5.09	4.84	5.46	6.33	5.80	5.28
^3S	5.62	5.57	6.52	6.86	6.59	6.45
^1S	6.36	6.34	7.05	7.59	7.26	6.78
^3P	6.44	6.43	7.31	7.68	7.43	7.29
^1P	6.83	6.77	7.48	8.07	7.75	7.46
^3S	7.16	7.15	8.02	8.40	8.12	8.00
^1S	7.34	7.33	8.13	8.58	8.31	8.09

a) Reference 76.

b) The effective Hamiltonian is calculated using the CCSD model.

c) Results are obtained from the partitioning of the EOM-CCSD matrix which comprises all singly and doubly excited determinants.

d) Reference 77.

e) A triplet instability.

Note All calculations for this table were performed with the 27 CGTO basis set listed in reference 76.

CHAPTER 8
CONCLUSIONS

The optimum structures of triazene, triimide, and triaziridine have been determined for the DZ basis set and the DZP basis set at the SCF level and for the DZP basis set at the MBPT(2) level of electron correlation. Relative electronic energies have been obtained with SDTQ-MBPT(4) and CCSD augmented by T(CCSD). Vibrational analyses of these structures have been carried out at all three levels of theory, showing that the optimum structures are true minima on the N_3H_3 potential energy surface. In addition, I have predicted infrared spectra of the important isomers using electron correlation. The vibrational frequencies and moments of inertia have also been used to compute thermochemical properties of the molecules, including the free energy.

Experimental and theoretical evidence suggests that some of these molecules can be isolated at room temperature. Low-temperature isolation of these compounds would very likely succeed. The predicted infrared spectra and thermochemical properties should aid experimental attempts to synthesize and isolate these compounds.

I feel that I now have a good understanding of the relative thermodynamic stabilities of the N_3H_3 molecules, but more work must be done in order to understand the kinetic lability of these compounds. Transition states need to be found to assess the kinetic stability of the various N_3H_3 isomers. Nguyen et al. claim to have found a variety of transition states on the N_3H_3 surface at the SCF level, but their

description of the search routine leads me to believe their transition structures are not necessarily points of zero force on the surface. Correlated geometry searches for transition states with subsequent frequency calculations will be needed to predict barrier heights and reaction pathways.

In addition to the N_3H_3 study, an approach for calculating vertical excitation energies using a coupled-cluster effective Hamiltonian has been derived using the equation-of-motion formalism. Only an initial implementation of this method has been achieved so far, but first results look promising. Excitation energies calculated with just an approximation to the full CISD matrix representation of $\bar{H}_N$ are markedly better than traditional TDA and RPA values and compare well with a multi-reference coupled-cluster scheme for nitrogen. However, RPA results calculated from an AGP reference were better for most of the states of beryllium that were investigated.

Obviously, the next step is to implement the effective Hamiltonian method at a higher level. The full EOM-CCSD matrix comprising all singly and doubly excited determinants needs to be computed, and spatial symmetry needs to be incorporated to allow the routine treatment of larger systems. Also, the inclusion of the three-body terms could have an effect. In the similar method of Mukherjee and Mukherjee, they report that three-body terms have little effect on numerical results,[70] but certain contributions from the three-body component of $\bar{H}_N$ in the present work would appear at low orders in perturbation theory if the equations for the coupled-cluster effective Hamiltonian are iterated order by order.

REFERENCES

1. C.C.J. Roothaan, Rev. Mod. Phys. 23, 69 (1951).

2. I. Shavitt, in Methods of Electronic Structure Theory, edited by H.F. Schaefer III (Plenum Press, New York, 1977), p. 189, and references therein.

3. A.C. Wahl and G. Das, in Methods of Electronic Structure Theory, edited by H.F. Schaefer III (Plenum Press, New York, 1977), p. 51, and references therein.

4. R. Shepard, in Advances in Chemical Physics Vol. 69, edited by K.P. Lawley (John Wiley and Sons Ltd., New York, 1987), p. 63, and references therein.

5. R.J. Bartlett and D.M. Silver, Phys. Rev. A10, 1927 (1974).

6. R.J. Bartlett and I. Shavitt, Chem. Phys. Lett. 50, 190 (1977); 59, 157 (1978); R.J. Bartlett, I. Shavitt and G.D. Purvis, J. Chem. Phys. 68, 2114 (1978).

7. S. Kucharski and R.J. Bartlett, Adv. Quantum Chem. 18, 281 (1986).

8. R.J. Bartlett and G.D. Purvis, Int. J. Quantum Chem. 14, 561 (1978).

9. J.A. Pople, R. Krishnan, H.B. Schlegel and J.S. Binkley, Int. J. Quantum Chem. 14, 545, (1978).

10. R.J. Bartlett, Annu. Rev. Phys. Chem. 32, 359 (1981).

11. F. Coester, Nucl. Phys. 1, 421 (1958); F. Coester and H. Kummel, Nucl.Phys. 17, 477 (1960).

12. J. Cizek, J. Chem. Phys. 45, 4256 (1966); Adv.Chem.Phys. 14, 35 (1969).

13. R.J. Bartlett, I. Shavitt and G.D. Purvis, J. Chem. Phys. 71, 281 (1979).

14. R.J. Bartlett and G.D. Purvis, Phys. Scripta 21, 255 (1980).

15. G.D. Purvis and R.J. Bartlett, J. Chem. Phys. 76, 1910 (1982).

16. R.J. Bartlett, H. Sekino, and G.D. Purvis III, Chem. Phys. Lett. 98, 66 (1983).

17. R.J. Bartlett, C.E. Dykstra and J. Paldus, in Advanced Theories and Computational Approaches for the Electronic Structure of Molecules, ed. C.E. Dykstra (Reidel, Dordecht, Holland 1984).

18. Y.S. Lee, S. Kucharski and R.J. Bartlett, J. Chem. Phys. 81, 5906 (1984).

19. J. Noga and R.J. Bartlett, J. Chem. Phys. 86, 7041 (1987).

20. T.H. Dunning and V. McKoy, J. Chem. Phys. 47, 1735 (1967), and references therein.

21. C. Møller and M.S. Plesset, Phys. Rev. 46, 618 (1934).

22. J. Oddershede, in Advances in Chemical Physics Vol. 69., edited by K.P. Lawley (John Wiley and Sons Ltd., New York, 1987), p. 201, and references therein.

23. R.A. Ferrel and T.T. Quinn, Phys. Rev. 108, 570 (1957).

24. D.J. Thouless, Nucl. Phys. 22, 78 (1961).

25. R.A. Ferrel, Phys. Rev. 107, 1631 (1957).

26. M.A. Ball and A.D. McLachlan, Mol. Phys. 7, 501 (1964).

27. A.E. Hansen and T.D. Bouman, Mol. Phys. 37, 1713 (1979).

28. T. Shibuya and V. McKoy, Phys Rev A 2, 2208 (1970).

29. D.H. Magers, R.J. Harrison, and R.J. Bartlett, J. Chem. Phys. 84, 3284 (1986).

30. S.J. Cole, G.D. Purvis, and R.J. Bartlett, Chem. Phys. Lett. 113, 271 (1985).

31. Bamford and Tipper, Comprehensive Chemical Kinetics Vol. 5, 1972, Elsevier Publishing Company.

32. Y. Kim, J.W. Gilje, and K. Seff, J. Am. Chem. Soc. 99, 7057 (1977).

33. C. Leuenberger, L. Hoesch, and A. Dreiding, J.C.S. Chem. Comm. 24, 1197 (1980); L. Hoesch, C. Leuenberger, H. Hilpert, and A. Dreiding, Helv. Chim. Acta 65, 2682 (1982).

34. W.C.E. Higginson and D. Sutton, J. Chem. Soc., 1042 (1953); J.W. Cahn and R.E. Powell, J. Am. Chem. Soc. 76, 2558 (1954); W.C.E. Higginson and P. Wright, J. Chem Soc., 155 (1955); W.C.E. Higginson, Chem. Soc. Spec. Publ. No. 10, 95 (1957); F. Bottomley, Q. Rev. Chem. Soc. 24, 617 (1970).

35. B.H.J. Bielski and J.W. Sutherland, IV International Congress on Radiation Research, Abs. No. 88 (1970); P.B. Pagsberg, IV International Congress on Radiation Research, Abs. No. 641 (1970); E. Hayon and M. Simic, J. Am. Chem. Soc. 94, 42 (1972); J.W. Sutherland, J. Phys. Chem. 83, 789 (1979).

36. W.A. Lathan, L. Radom, P.C. Hariharan, W.J. Hehre, and J.A. Pople, Topics Current Chem. 40, 1 (1973).

37. J.M. Howell and L.J. Kirschenbaum, J. Am. Chem. Soc. 98, 877 (1976).

38. P.C. Hiberty and C. Leforestier, J. Am. Chem. Soc. 100, 2012 (1978).

39. B.M. Gimarc and N. Trinajstić, Pure Appl. Chem. 52, 1443 (1980).

40. S.D. Peyerimhoff and R.J. Buenker, J. Chem. Phys. 47, 1953 (1967); P.J. Hay, and W.A. Goddard III, Chem. Phys. Lett. 14, 46, (1972); J.S. Wright, Can. J. Chem. 51, 139 (1973); A.K.Q. Siu and E.F. Hayes, Chem. Phys. Lett. 21, 573 (1973); P.J. Hay, T.H. Dunning, and W.A. Goddard III, Chem. Phys. Lett. 23, 457 (1973); S. Shih, R.J. Buenker, and S.D. Peyerimhoff, Chem. Phys. Lett. 28, 463 (1974).

41. R.R. Lucchese and H.F. Schaefer III, J. Chem. Phys. 67, 2290 (1977); G. Karlstrom, S. Engstrom, and B. Jonsson, Chem. Phys. Lett. 57, 390 (1978).

42. L.B. Harding and W.A. Goddard, J. Chem Phys. 67, 2377, (1977).

43. M.T. Nguyen, J. Kaneti, L. Hoesch, and A.S. Dreiding, Helv. Chim. Acta 67, 1918 (1984).

44. C. Salter, Ph.D. Dissertation, Vanderbilt University (1986).

45. J. Garrett and I.M. Mills, J. Chem. Phys. 49, 1719 (1968); P. Pulay, Mol. Phys. 17, 197 (1969); 18, 473 (1970); K. Thompson and P. Swanstrom, Mol. Phys. 26, 735 (1973).

46. J.A. Pople, R. Krishnan, H.B. Schlegel, and J.S. Binkley, Int. J. Quantum Chem. S13, 255 (1979).

47. N.C. Handy, R.D. Amos, J.F. Gaw, J.E. Rice and E.S. Simandiras, Chem. Phys. Lett. 120, 151 (1985); R.J. Harrison, G.B. Fitzgerald, W.D. Laidig, and R.J. Bartlett, Chem. Phys. Lett. 124, 291 (1986); N.C. Handy, R.D. Amos, J.F. Gaw, J.E. Rice, E.D. Simandrias, T.J. Lee, R.J. Harrison, W.D. Laidig, G.B. Fitzgerald, and R.J. Bartlett, in Geometrical Derivatives of Energy Surfaces and Molecular Properties, ed. P. Jørgensen and J. Simons, Reidel, Dordrecht, The Netherlands, 179 (1986).

48. G.B. Fitzgerald, S.J. Cole, and R.J. Bartlett, J. Chem. Phys. 85, 1701 (1986).

49. S.J. Cole and R.J. Bartlett, J.Chem. Phys. 86, 873 (1987).

50. J.F. Stanton, W.N. Lipscomb, D.H. Magers, and R.J. Bartlett, J. Chem. Phys., in press.

51. T.H. Dunning, Jr., J. Chem. Phys. 53, 2823, (1970).

52. L.T. Redmon, G.D. Purvis III, and R.J. Bartlett, J. Am. Chem. Soc. 101, 2856 (1979).

53. ACES (Advanced Concepts in Electronic Structure) ab initio program system: R.J. Bartlett, G.D. Purvis, G.B. Fitzgerald, R.J. Harrison, Y.S. Lee, S.A. Kucharski, H. Sekino, W.D. Laidig, S.J. Cole, D.H. Magers, E.A. Salter, G.W. Trucks, D.E. Bernholdt, C. Sosa, M. Rittby, S. Pal, J. Watts, J. Noga, and J.F. Stanton. This program system performs SCF, MBPT, and CC calculations for electronic energies of molecules. Correlated calculations may be performed with RHF, ROHF, UHF, and other reference functions. The program also performs analytical first derivative calculations at the SCF level and at various levels of MBPT and CC theory. It currently performs analytical second derivative calculations at the SCF and MBPT(2) levels. Additional options in the program allow the prediction of excitation and ionization processes using CC/MBPT theory. Currently the ACES programs employ J. Almloef's MOLECULE and R. Pitzer's integral packages.

54. L.J. Schaad, C.S. Ewig, B.A. Hess, Jr., and D. Michalska, J. Chem. Phys. 83, 5348 (1985).

55. W.A. Goddard III, T.H. Dunning, W.J. Hunt, and P.J. Hay, Acc. Chem. Res. 6, 368 (1973).

56. P.J. Hay, T.H. Dunning, and W.A. Goddard III, J. Chem. Phys. 62, 3912 (1975).

57. W.D. Laidig and H.F. Schaefer III, J. Chem. Phys 74, 3411 (1981).

58. R.C. Ladner and W.A. Goddard III, J. Chem. Phys. 51, 1073 (1969); W.A. Goddard III and R.C. Ladner, J. Am. Chem. Soc. 93, 6750 (1971); W.J. Hunt, P.J. Hay, and W.A. Goddard III, J. Chem. Phys. 57, 738 (1972).

59. PLOTGIBB: C. Salter, E.A. Salter, and D.H. Magers. This program calculates thermochemical quantities using ordinary statistical thermodynamic partition functions. The only input required is the geometry of the molecule and the vibrational frequencies.

60. Y. Yamaguchi, M. Frisch, J. Gaw, H.F. Schaefer III, J.S. Binkley, J. Chem. Phys. 84, 2262 (1986).

61. E.F. Hayes and A.K.Q. Siu, J. Am. Chem. Soc. 93, 2090 (1971).

62. M.A. Natiello, H.F. Reale, and J.A. Medrano, J. Comp. Chem. 6, 108 (1985).

63. T. Tanaka and Y. Morino, J. Mol. Spect. 33, 538 (1970); M. Lichtenstein, J.J. Gallagher, and S.A. Clough, J. Mol. Spect. 40, 10 (1971).

64. G. Herzberg, Spectra of Diatomic Molecules, 1950, Van Nostrand Reinhold Company Inc., New York.

65. K. Kuchitsu, J.P. Guillory, and L.S. Bartell, J. Chem. Phys. 49, 2488 (1968).

66. W.S. Benedict and E.K. Plyler, Can. J. Phys. 35, 1235 (1957).

67. Tables of Vibrational Frequencies, ed. T. Shimanouchi, National Bureau of Standards Natl. Stand. Data Serv. Natl. Bur. Stand. 39 (U.S. GPO, Washington, D.C., 1972), Vol. 1.

68. D.J. Rowe, Rev. Mod. Phys. 40, 153 (1968).

69. F.E. Harris, Int. J. Quantum Chem. Symp. 11, 403 (1977).

70. D. Mukherjee and P.K. Mukherjee, Chem. Phys. 39, 325 (1979).

71. S. Ghosh, D. Mukherjee, ans S.N. Bhattacharyya, Chem. Phys. 72, 161 (1982), Mol. Phys. 43, 173 (1981); S.S.Z. Adnan, S. Bhattacharyya, and D. Mukherjee, Chem. Phys. Lett. 85, 204 (1982).

72. H. Sekino and R.J. Bartlett, Int. J. Quantum Chem. Symp. 18, 255 (1984).

73. W.D. Laidig and R.J. Bartlett, Chem. Phys. Lett. 104, 424 (1984).

74. S. Pal, M. Rittby, R.J. Bartlett, D. Sinha, and D. Mukherjee, J. Chem. Phys. 88, 4357 (1988).

75. E.S. Nielsen, P. Jørgensen, and J. Oddershede, J. Chem. Phys. 73, 6238 (1980).

76. R.B. RoyChowdhury, Ph.D. Dissertation, University of Florida (1985).

77. H.E. White, Introduction to Atomic Spectra, (McGraw-Hill, New York, 1934), p. 179.

BIOGRAPHICAL SKETCH

David Huey Magers was born on November 23, 1960, to Mr. and Mrs. Hughey M. Magers. He has one older sister, Sylvia. He lived in Bentonia, Mississippi, until leaving to attend college at Mississippi College (M.C.) in Clinton, Mississippi in the fall of 1978. David received his Bachelor of Science degree in chemistry with a minor in Physics from M.C. in the spring of 1982 and graduated summa cum laude with high honors in his undergraduate research project. During his senior year he was awarded the Joseph Barnhill Memorial Award as the top graduate in chemistry, and upon graduation David received the Nelson Scholar Award for having the highest grade point average in his graduating class. In the fall of 1982, he began his graduate work at the University of Florida.

In April of 1983, David married Tina Lynn Godwin of Pensacola, with whom he had gone to college at M.C. Tina is a critical-care registered nurse. In August of 1986 their son David Brandon Magers was born. Brandon has red hair just like his father's. David loves his Lord and his family, and tries to put them first even in the hectic life of graduate school.

David enjoys most sports, but basketball tops the list. He played varsity basketball and baseball in high school. David is also a percussionist. He played in marching, concert, and jazz bands

throughout high school and college. Watching movies, eating chocolate, and arguing about politics are among David's other favorite activities.

I certify that I have read this study and that in my opinion it conforms to acceptable standards of scholarly presentation and is fully adequate, in scope and quality, as a dissertation for the degree of Doctor of Philosophy.

Rodney J. Bartlett, Chairman
Professor of Chemistry

I certify that I have read this study and that in my opinion it conforms to acceptable standards of scholarly presentation and is fully adequate, in scope and quality, as a dissertation for the degree of Doctor of Philosophy.

Michael C. Zerner
Professor of Chemistry

I certify that I have read this study and that in my opinion it conforms to acceptable standards of scholarly presentation and is fully adequate, in scope and quality, as a dissertation for the degree of Doctor of Philosophy.

David A. Micha
Professor of Physics and Chemistry